Looking at the "Water-in-Deep-Eutectic-Solvent" System: A Dilution Range for High Performance Eutectics

Nieves López-Salas,[a,*] José Manuel Vicent-Luna,[b] Silvia Imberti,[c] Elena Posada,[a] María Jesús Roldán,[a] Juan Anta,[b] Salvador Balestra,[b] Rafael María Madero Castro,[b] Sofia Calero,[b] Rafael Jiménez-Riobóo,[a] María Concepción Gutiérrez,[a] María Luisa Ferrer,[a] and Francisco del Monte[a,*]

[a] Materials Science Factory, Instituto de Ciencia de Materiales de Madrid-ICMM, Consejo Superior de Investigaciones Científicas-CSIC. C/ Sor Juana Inés de la Cruz, 3. Campus de Cantoblanco, 28049-Madrid (Spain) E-mail: delmonte@icmm.csic.es / marialasnieves.lopez@gmail.com, [b] Department of Physical, Chemical, and Natural Systems, Universidad Pablo de Olavide, Ctra. Utrera km. 1, ES-41013 Seville, Spain, [c] STFC, Rutherford Appleton Laboratory, Didcot, UK

Number of pages: 40
Number of figures: 26
Number of schemes: 0
Number of tables: 8
Number of equations: 6

Experimental part

Materials

Resorcinol (R), urea (U) and choline chloride (ChCl) were purchased from Sigma-Aldrich and used as received. Water was distilled and deionized.

DES and DES dilutions preparation

RUChCl DES was obtained by physical mixing of the individual components (R, U and ChCl in a 3:2:1 molar ratio) followed by a thermal treatment at 90 °C (see reference 33 in main text for further details). RUChCl-W dilutions (water contents of 15, 25, 35, 50, 60 and 75 wt%) were prepared by physical mixing of the DES and the corresponding water amount at room temperature.

Sample characterization

Densities, viscosities and ultrasonic velocities were measured in a DSA 5000M coupled with a LOVIS 2000 ME module from Anton Paar. Differential scanning calorimetry (DSC) analyses were performed in a TA Instruments Discovery system under a N_2 atmosphere. The samples were sealed in an aluminium pan and placed in the calorimeter furnace. For data acquisition, DESs were cooled from room temperature to -90 °C at a scan rate of 5 °C min^{-1} and kept at this temperature over 10 min before starting the heating/cooling cycle, which consisted of heating the sample to 80 °C and then cooling it again to -90 °C at the same scan rate. The cycle measurement was repeated three times. Thermogravimentrical analyses (TGA) were carried out in a TA Instruments TGA Q500. The samples were placed inside an aluminium pan in a sealed furnace and heated at 10 °C min^{-1} from room temperature to 250 °C in a N_2 atmosphere.

Brillouin spectroscopy

Brillouin spectra were recorded using a Sandercock 3 + 3 Pass Tandem Fabry-Pérot interferometer as Brillouin spectrometer and the light source was a DPPS laser working at a wavelength (λ_0) of 532 nm.[1] In this case, the liquid samples were placed in optical cuvettes (Starna) with 1 mm in optical path length. Experiments were performed using backscattering and 90 A scattering geometry, simultaneously.

The simultaneous recording of both scattering geometries required of the use of a neutral filter for the Backscattering component and we also had to reduce the intensity of the central peak. The Brillouin peaks were fitted using a Lorentzian function with an adequate background function. The

constraints associated with this experimental set-up made impossible the application of a typical damped harmonic oscillator model.

The 90A scattering geometry is independent of the refractive index (n)[2] and its acoustic wave vector is

$$q^{90A} = [4\pi\sin(\pi/4)] / \lambda_0 \quad \text{(S1)}$$

The hypersonic sound propagation velocity (v_H) can be obtained from the relation between the Brillouin frequency shift (f^{90A}) and q^{90A}, and expressed as

$$v_H^{90A} = (2\pi f^{90A}) / q^{90A} \quad \text{(S2)}$$

Meanwhile, the acoustic wave vector for Backscattering geometries is

$$q^{180} = [4\pi n] / \lambda_0, \quad \text{(S3)}$$

and hence n-dependent. Thus, the hypersonic velocities for both geometries are:

$$v_H^{90A} = f^{90A}\lambda_0 / \sqrt{2} \; ; \; v_H^{180} = f^{180}\lambda_0 / 2n \quad \text{(S4)}$$

NMR analysis

^{1}H NMR spectra were recorded using a Bruker Avance DRX500 spectrometer operating at 500 MHz with a 30° pulse, acquisition time of 3.1719 s, relaxation delay of 1 s and 16 scans. The samples were placed in 5 mm NMR glass tubes with a height of 8 in and dimethylsulfoxide (DMSO‑d6) – used as the external reference – was placed in a coaxial tube. The peaks were identified and spectra were processed using the software MestReNova. ^{1}H NMR diffusion experiments were performed using a pulsed-field gradient stimulated spin-echo (PFG-STE NMR) technique by applying a LED-bipolar gradients pulse sequence from Bruker (in particular, ledbpgp2s pulse sequence)[3]. The spectrometer was equipped with a broadband fluorine observe (BBFO) NMR probe capable of producing magnetic fields pulses in the z-direction. A Bruker Variable Temperature BVT 3000 was also used to set the temperature to 353 K for the measurements of samples at temperature different of RT.

The NMR signal attenuation (I/I_0) is described by the equation:[4]

$$I = I_0\, e^{-D\gamma^2 g^2 \delta^2 (\Delta - \frac{\delta}{3})} \quad \text{(S5)}$$

Or in a simplified form

$$I = I_0\, e^{-DQ} \quad \text{(S6)}$$

where, I is the observed intensity, I_0 is the intensity when the gradient strength is zero (reference intensity), D is de diffusion coefficient, γ is the gyromagnetic ratio of the observed nuclei, g is the gradient strength, δ is the duration of the gradient and Δ is the diffusion time.

The gyromagnetic ratio is different for every nucleus, being 4.3 kHz G^{-1} for ^1H. The duration of the gradient and the diffusion time differ among samples. NMR data used to obtain these data are shown in Fig. S24 and S25, and Tables S6, S7 and S8.

The software MestReNova was used for the diffusion coefficients calculation by the peak integration and fitting of the exponentially decaying data based on the area.

Neutron diffraction experiments

Hydrogenated resorcinol, urea, choline chloride and deuterated water (99.9%-d2) were purchased from Sigma-Aldrich and used as received. d9-choline chloride ($(CD_3)_3N(CH_2)_2OHCl$, 98.8%-d9) was acquired from CIL laboratories. d4-urea (97.0%-D4) and d6-resorcinol (65.0%-D6) were prepared by ISIS Deuteration Facility. Different isotopic substitution RUChCl samples were prepared by mixing the appropriate amount of the fully protonated and deuterated compounds and letting the mixture melt at 80 °C. The different isotopic contrasts are summarized in Table S2.

Neutron diffraction experiments were collected using the NIMROD diffractometer, located in Target Station 2 in the ISIS Neutron and Muon Facility, Rutherford Appleton Laboratories, Harwell Campus, UK. Neutron scattering data were recorded placing each freshly prepared solution into 1mm thickness flat TiZr alloy cans. Samples were kept at 353 K using a circulating heater to ensure the DES remained in liquid phase during the whole data collection time.

Empirical potential structure refinement (EPSR)[5] and EPSRgui[6] were used to obtain computational models of the different systems. EPSR algorithm minimizes the system energy and, at the same time, builds an atomistic model that fits the collected data. Previous to be used in EPSR algorithm, neutron scattering data were treated using GudrunN in order to correct them according to detectors efficiency, subtract environment background, multiple scattering, and hydrogen inelastic scattering.[7] Final datasets were then analyzed using EPSR that allowed to maximize the information obtained from them and allows comparing data with conventional simulations. The assigned bond lengths and atom types used to build the atomistic models are described in Table S3. Urea and choline chloride charges, masses and Lennard-Jones parameters used were the same

as in reference #7.[8] Resorcinol Lennard-Jones parameters were adapted from Jorgensen[9] and masses and charges extracted from reference #9.[10] The simulation boxes contain 7000 molecules, at the density of 0.1 atoms/Å^3.

Molecular dynamics simulations

Molecular dynamics (MD) simulations were performed to study the structural and transport properties of the DES RUChCl in presence of water. The molecular models for the molecules of urea, choline, and chloride are taken from Perkins et al.[11] In that work, the authors stated that the developed force field reproduces the physico-chemical properties of the urea/choline chloride DES, and in particular density, volume expansion coefficient, heat capacity and diffusion coefficients. We use OPLS-AA force field[8, 12] for resorcinol HBD, and SPC/E model for water.[13] To calculate the cross Lennard-Jones potential parameters we use standard Lorentz-Berthelot combining rules. The Lennard-Jones cut-off radius is set to 12 Å and electrostatic interactions are computed using the Ewald summation technique.[14, 15] We applied periodic boundary conditions in the three dimensions.

Different concentrations covering the whole range from the pure solvent to the pure RUChCl with eleven intermediate weight percentages of RUChCl were studied. The components of the mixtures were initially placed in a cubic simulation box of approximately 40 Å. The number of ion pairs and organic compounds of each system, as well as the total number of atoms are shown in the Table S4. The initial configurations were created by randomly placing the RUChCl constituents in an empty simulation box and refilled with water molecules using the Packmol package,[16] thus obtaining a homogeneous distribution of the molecules. We started the equilibration of the system by performing an energy minimization simulation employing a steepest descent algorithm.[17] We continued with consecutive MD simulations in the NPT ensemble to relax the systems to their equilibrium density. This equilibrium is reached when the cell volume and the energy of the system fluctuate around an average value over time. Once the system was equilibrated we carried out MD simulations in the NVT ensemble to obtain the rest of the structural and dynamical properties of the RUChCl aqueous dilutions. The time step employed for the equilibration and production run simulations is 0.5 and 1 fs, respectively. The production runs consists in 50 million of MD steps giving rise to 50 ns of total simulation time. The pressure in the NPT simulations was set using the Martyna-Tuckerman-Tobias-Klein (MTTK) barostat,[18] and the temperature was controlled with the Nose-Hoover thermostat.[19,20] All simulations were performed using the GROMACS molecular simulation software.[21-24]

Self-diffusion coefficients D_s were computed using Einstein's equation that relates D_s with the slope of the mean square displacement in the 10-40 ns time interval. Additional details about the calculation of the transport properties of liquid systems can be found elsewhere (for further details see references[25, 26] and also reference 45 in main text). For the calculation of hydrogen bonds we used the geometric criterion described by Luzar and Chandler[27] over the trajectory recorded every 0.1 ns.

Table S1 – Summary molar and wt% composition of the prepared samples.

Name	DES (mol)	Water (mol)[a]	wt% of DES
RUChCl0W	1	0	100
RUChCl6W	1	6	85
RUChCl11W	1	11	75
RUChCl18W	1	18	65
RUChCl32W	1	32	50
RUChCl49W	1	49	40
RUChCl97W	1	97	25

[a] number of moles of water is 'n' along the paper

Table S2 – Summary of the different isotopic substitution used in RUChCl0W, RUChCl11W, RUChCl32W, and RUChCl97W to carry out neutron scattering experiments.

Sample H/D substitutions															
RUChCl0W (100wt% of DES)				RUChCl11W (75wt% of DES)				RUChCl32W (50wt% of DES)				RUChCl97W (25wt% of DES)			
R 3	**U 2**	**ChCl 1**	**W 0**	**R 3**	**U 2**	**ChCl 1**	**W 11**	**R 3**	**U 2**	**ChCl 1**	**W 32**	**R 3**	**U 2**	**ChCl 1**	**W 97**
D	D	D	-	D	D	D	D	D	D	D	D	D	D	D	D
H	D	D	-	H	D	D	D	H	D	D	D	H	D	D	D
D	H	D	-	D	H	D	D	D	H	D	D	D	H	D	D
D	D	H	-	D	D	H	D	D	D	H	D	D	D	H	D
H	H	H	-	D	D	D	H	D	D	D	H	D	D	D	H
DH	DH	HD	-	H	H	H	H	H	H	H	H	H	H	H	H
DH	D	D	-	DH	DH	HD	DH	DH	DH	HD	DH	DH	DH	HD	DH
D	DH	D	-	DH	D	D	D	DH	D	D	D	DH	D	D	D
D	D	DH	-	D	DH	D	D	D	DH	D	D	D	DH	D	D
				D	D	DH	D	D	D	DH	D	D	D	DH	D
				D	D	D	DH	D	D	D	DH	D	D	D	DH

* "DH" consists on a 50wt% mixture of H and D isotopes of the correspondent molecule. From this point on, it will be abbreviated as "M".

Table S3 – Lennard-Jones parameters, masses, and point charges used in the reference potential to simulate RUChCl DES components and water. Atom types are depicted in Figure 1 of the manuscript.

	Atom type	ε (kJ/mol)	σ (Å)	mass (amu)	q (e)
Resorcinol	Cr5	0.293	3.550	12.011	0.098
	Cr4	0.293	3.550	12.011	-0.589
	Hr5	0.126	2.420	2.000	0.133
	Cr1	0.293	3.550	112.010	0.601
	Hr4	0.126	2.420	2.000	0.198
	Cr2	0.293	3.550	112.010	-0.585
	Or	0.711	3.070	15.999	-0.622
	Hr2	0.126	2.420	2.000	0.266
	Hrp	0.000	0.000	2.000	0.456
Urea	Cu	0.439	3.750	12.011	0.152
	Ou	0.878	2.960	15.999	-0.390
	Nu	0.711	3.250	14.007	-0.541
	Hu	0.000	0.000	2.000	0.330
Choline	Nc	0.700	3.200	14.007	1.000
	Cc4	0.800	3.700	12.011	-0.120
	Cc1	0.800	3.700	12.011	-0.180
	Cc5	0.800	3.700	12.011	0.145
	Hc4	0.200	2.580	2.000	0.060
	Hc1	0.200	2.580	2.000	0.060
	Oc	0.650	3.100	15.999	-0.683
	Hc5	0.200	2.580	2.000	0.060
	Hco	0.000	0.000	2.000	0.418
Chloride	Cl	0.566	4.191	35.453	-1.000
Water	HW	0.000	0.000	2.000	0.423
	OW	0.650	3.166	16.000	-0.847

Table S4 – Number of molecules/ion pairs and number of atoms in the simulation box for MD simulations.

Number of molecules/ion pairs					
RUChCl (wt%)	**Resorcinol**	**Urea**	**Choline Chloride**	**Water**	**Total**
10	18	12	6	2263	2299
25	54	36	18	1886	1994
40	90	60	30	1509	1689
55	126	84	42	1131	1383
60	138	92	46	1006	1282
65	144	96	48	880	1168
70	156	104	52	754	1066
75	168	112	56	628	964
80	180	120	60	503	863
85	192	128	64	377	761
90	204	136	68	251	659
100	228	152	76	0	456

Number of atoms					
RUChCl (wt%)	**Resorcinol**	**Urea**	**Choline Chloride**	**Water**	**Total**
10	252	96	127	6789	7264
25	756	288	379	5658	7081
40	1260	480	631	4527	6898
55	1764	672	883	3393	6712
60	1932	736	967	3018	6653
65	2016	768	1009	2640	6433
70	2184	832	1093	2262	6371
75	2352	896	1177	1884	6309
80	2520	960	1261	1509	6250
85	2688	1024	1345	1131	6188
90	2856	1088	1429	753	6126
100	3192	1216	1597	0	6005

Table S5 – Coordination numbers around electronegative centers as obtained from EPSR analysis of neutron scattering experiments.

	Atom		r_{coord}			Ncoord											
RDF	A	B	**(*Å*)**			**RUChCl0W**			**RUChCl11W**			**RUChCl32W**			**RUChCl97W**		
R-R	Or	Hrp	1.0	-	2.5	0.68	±	0.65	0.16	±	0.39	0.10	±	0.30	0.04	±	0.19
U-R	Or	Hu	1.0	-	2.5	0.29	±	0.52	0.17	±	0.40	0.08	±	0.29	0.04	±	0.20
Ch-R	Or	Hco	1.0	-	2.5	0.03	±	0.18	0.01	±	0.09	0.01	±	0.11	0.01	±	0.10
W-R	Or	Hw	1.0	-	2.5		-		0.49	±	0.64	0.71	±	0.71	0.90	±	0.73
R-U	Ou	Hrp	1.0	-	2.9	0.61	±	0.73	0.41	±	0.58	0.16	±	0.38	0.12	±	0.33
U-U	Ou	Hu	1.0	-	2.9	2.84	±	1.21	2.51	±	0.84	2.43	±	0.75	2.15	±	0.54
Ch-U	Ou	Hco	1.0	-	2.9	0.09	±	0.29	0.05	±	0.22	0.04	±	0.20	0.01	±	0.12
W-U	Ou	Hw	1.0	-	2.9		-		1.42	±	1.26	2.25	±	1.32	2.97	±	1.31
R-Cl	Cl	Hrp	1.3	-	2.6	1.32	±	0.88	0.77	±	0.78	0.44	±	0.55	0.30	±	0.47
U-Cl	Cl	Hu	1.3	-	2.6	0.99	±	1.00	0.53	±	0.68	0.35	±	0.54	0.18	±	0.40
Ch-Cl	Cl	Hco	1.3	-	2.6	0.32	±	0.54	0.38	±	0.56	0.19	±	0.44	0.15	±	0.39
W-Cl	Cl	Hw	1.3	-	2.6		-		1.34	±	1.05	2.63	±	1.17	3.38	±	1.31
R-Ch	Oc	Hrp	1.0	-	2.5	0.24	±	0.45	0.16	±	0.39	0.13	±	0.34	0.02	±	0.14
U-Ch	Oc	Hu	1.0	-	2.5	0.30	±	0.50	0.24	±	0.45	0.11	±	0.34	0.06	±	0.23
Ch-Ch	Oc	Hco	1.0	-	2.5	0.54	±	0.56	0.03	±	0.17	0.02	±	0.14	0.00	±	0.06
W-Ch	Oc	Hw	1.0	-	2.5		-		0.34	±	0.56	0.65	±	0.77	1.06	±	0.73
R-W	Ow	Hrp	1.0	-	2.5		-		0.24	±	0.46	0.13	±	0.35	0.05	±	0.23
U-W	Ow	Hu	1.0	-	2.5		-		0.28	±	0.51	0.15	±	0.38	0.06	±	0.25
W-W	Ow	Hw	1.0	-	2.5		-		1.26	±	0.93	1.57	±	0.92	1.76	±	0.85
Ch-W	Ow	Hco	1.0	-	2.5		-		0.02	±	0.14	0.01	±	0.12	0.01	±	0.08
R-U	Nu	Hrp	1.3	-	4.4	2.30	±	1.39	1.54	±	1.12	0.79	±	0.85	0.40	±	0.64
U-U	Nu	Hu	1.3	-	4.4	5.29	±	2.56	4.13	±	1.93	3.64	±	1.77	2.59	±	1.10
Ch-U	Nu	Hco	1.3	-	4.4	0.34	±	0.55	0.20	±	0.45	0.15	±	0.39	0.06	±	0.24
U-W	Nu	Hw	1.3	-	4.4		-		6.92	±	3.56	12.05	±	3.80	15.62	±	3.80

Table S6 – Experimental parameters – e.g, diffusion time (Δ) and duration of the gradient (δ) – used for the diffusion coefficient calculations.

RUChCl sample (DES content in wt%)	**Δ (ms)**		**δ (ms)**	
	298 K	**353 K**	**298 K**	**353 K**
RUChCl0W (100 wt%)	900	400	8	4.4
RUCHCl6W (85 wt%)	500	200	4.4	2.2
RUChCl11W (75 wt%)	400	400	4	2
RUChCl18W (65 wt%)	400	200	4.4	2.2
RUChCl32W (50 wt%)	400	400	2.2	1.6
RUChCl97W (25 wt%)	400	300	2.2	1.1

Table S7 – Chemical shift (δ, ppm) of the ^{1}H NMR of the sample RUChCl 321 and water dilutions at room temperature.

	RUChCl sample (DES content in wt%)	Resorcinol				Urea	Choline Chloride			HDO
		OH	H at C5	H at C2	H at C4 & C6	H	H at -CH_2-OH	H at -CH_2-N	H at CH_3	
δ, ppm	RUChCl0W (100%)	7.43 (bs, 6H)	6.19 (bs, 3H)	5.83 (bs, 3H)	5.69 (bs, 6H)	5.05 (s, 8H)	2.87 (s, 2H)	2.01 (s, 2H)	1.71 (s, 9H)	------
	RUChCl6W (85%)	----	6.20 (m, 3H)	5.76 (bs, 3H)	5.68-5.66 (dd, 5.9H)	4.98 (s, 5H)	2.90 (m,2H)	2.08 (m, 2H)	1.79 (s, 9H)	5.39 (s,10.6H)
	RUChCl11W (75%)	----	6.23 (m, 3H)	5.75 (t, 3H)	5.69-5.67 (dd, 6H)	4.93 (s)	2.93 (m, 2H)	2.14 (m, 2H)	1.86 (s, 9H)	4.97 (s)
	RUChCl18W (65%)	----	6,26 (m, 3H)	5.74 (t, 3H)	5.69 (dd, 6H)	4,98 (s, 2.5H)	2.99 (m, 2H)	2.22 (m, 2H)	1.93 (s, 9H)	4.64 (s, 13H)
	RUChCl32W (50%)	----	6.31 (m, 3H)	5.72 (m, 8.7H)		5.00 (s, 1.5H)	3.05 (m, 2H)	2,32 (m, 2H)	2.04 (s, 9H)	4.40 (s, 14.2H)
	RUChCl97W (25%)	----	6.44 (m, 3H)	5.79 (m, 8.2H)		5.09 (s, 0.4H)	3.23 (m, 2H)	2.58 (m, 2H)	2.29 (s, 9H)	4.25 (s, 14.1H)

Table S8 – Chemical shift (δ, ppm) of the ^{1}H NMR of the sample RUChCl 321 and water dilutions at 80 °C.

	RUChCl sample (DES content in wt%)	Resorcinol				Urea	Choline Chloride			HDO
		OH	H at C5	H at C2	H at C4 & C6	H	H at -CH_2-OH	H at -CH_2-N	H at CH_3	
δ, ppm	RUChCl0W (100%)	7.09 (bs, 6H)	6.19 (t, 3H)	5.81 (d, 3H)	5.70 (dd, 6H)	4.80 (s, 7.7H)	2.92 (s, 2H)	2.12 (s, 2H)	1.82 (s, 9H)	------
	RUChCl6W (85%)	----	6.22 (t, 3H)	5.77 (bs, 2.8H)	5.69-5.67 (dd, 5H)	4.79 (s)	2.97 (m, 2H)	2.22 (m, 2H)	1.92 (s, 9H)	4.91 (s)
	RUChCl11W (75%)	----	6.25 (bs, 3H)	5.76 (bs, 1.8H)	5.70-5.68 (bd, 3.5H)	4.78 (s, 4H)	3.01 (m, 2H)	2.28 (m, 2H)	1.98 (s, 9H)	4.47 (s, 14.9H)
	RUChCl18W (65%)	----	6.29 (m, 3H)	5.76 (bs, 2.7H)	5.71 (dd, 5.1H)	4.81 (s, 2.4H)	3.07 (m, 2H)	2.35 (m, 2H)	2.06 (s, 9H)	4.16 (s, 14H)
	RUChCl32W (50%)	----	6.34 (m, 3H)	5.74 (m, 4.6H)		4.84 (s, 1.5H)	3.13 (m, 2H)	2,45 (m, 2H)	2.16 (s, 9H)	3.91 (s, 18.1H)
	RUChCl97W (25%)	----	6.45 (m, 2.5H)	5.81 (m, 1.1H)		4.93 (s, 0.5H)	3.29 (m, 2H)	2.66 (m, 2H)	2.35 (s, 9H)	3.74 (s, 19.4H)

Figure S1 - Experimental (data, black line) and EPSR-fitted (EPSR, blue line) scattered intensity as a function of (left) Q and (right) r space for in A) RUChCl0W, B) RUChCl11W, C) RUChCl32W, and D) RUChCl97W. EPSR fits of the total diffraction data shown as a function of (left) Q and (right) r space of RUChClW samples (please note that levels have been shifted in the Y-axes for clarity).

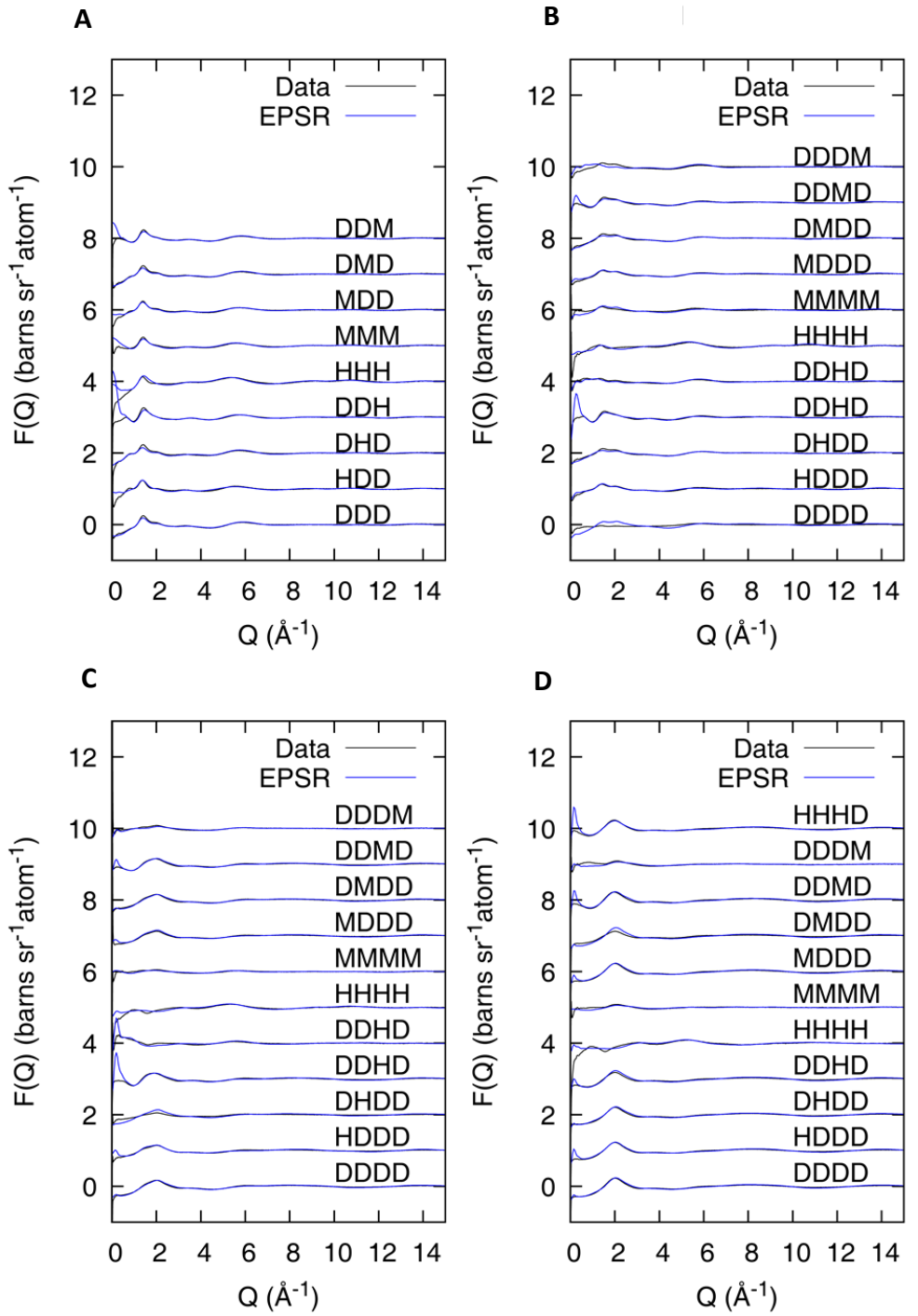

*The different contrasts are labeled acording to RUChCl*n*W isotopes. Note that H stands for the fully protonated isotope of a given molecule, D for the deuterated one whereas M stands for a 50wt% mixture of H and D compounds (e.g., DDDM stands for fully deuterated R, U and ChCl mixed with a 50wt% mixture of D/H isotopes of water).

Figure S2 – Experimental scattered intensity as a function of Q for RUChCl0W (red line), RUChCl11W (green line), RUChCl32W (blue line), and RUChCl97W (yellow line) to analyse the overall evolution of the solvents structure.

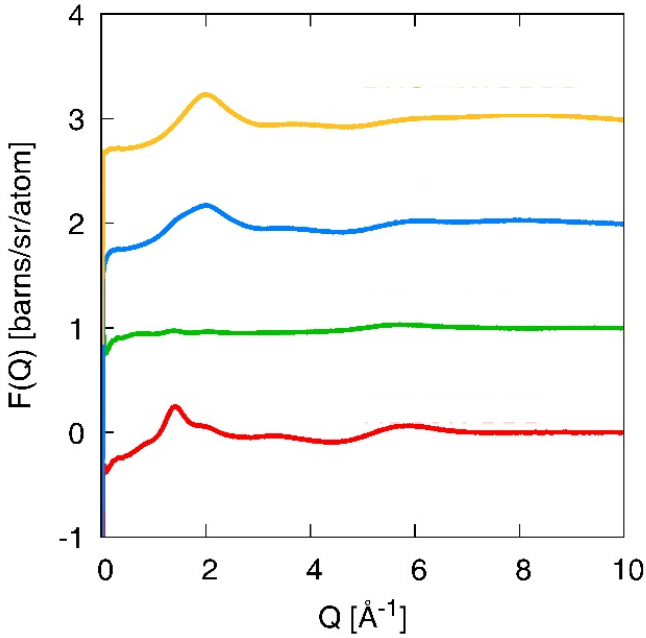

Figure S3 – EPSR-derived RDFs for pair correlations between resorcinol and all DES components in RUChCl0W (red line), RUChCl11W (green line), RUChCl32W (blue line), and RUChCl97W (yellow line).

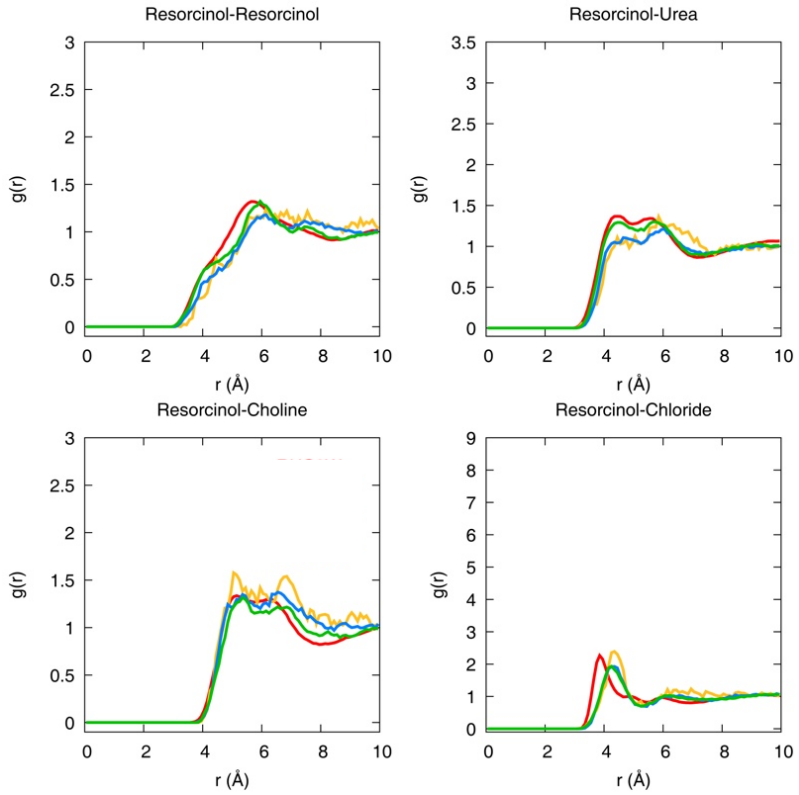

Figure S4 – Top panel: EPSR-derived partial RDFs for atom-atom pair correlations – i.e. between chloride and different urea atoms – in A) RUChCl0W, B) RUChCl11W, C) RUChCl32W, and D) RUChCl97W. **Bottom panel:** Partial RDFs obtained by Hammond et al. are included for comparison. Data were reproduced with permission from reference 29 of main text. Copyright ©, Royal Society of Chemistry.

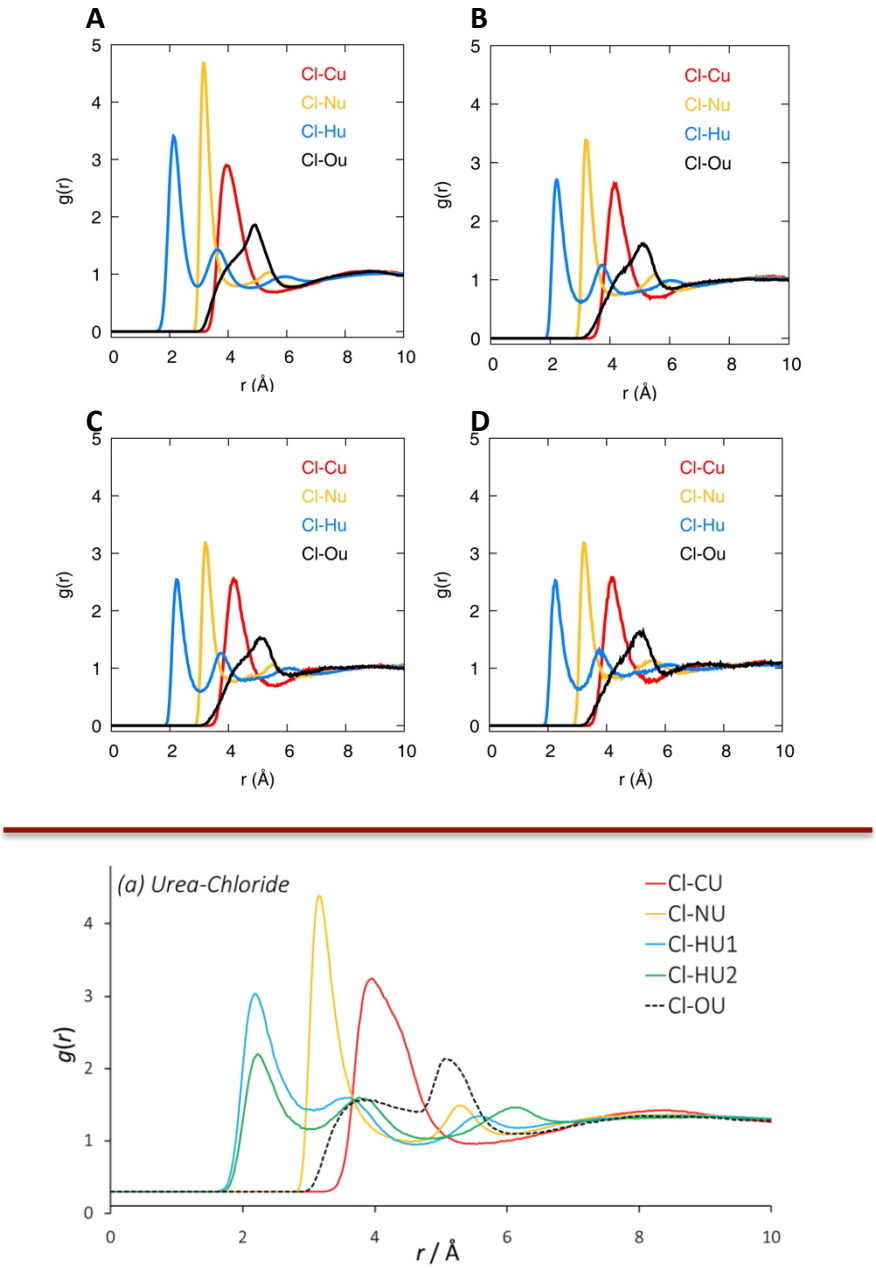

Figure S5 – Top panel: EPSR-derived partial RDFs for atom-atom pair correlations – i.e. between urea atoms – in A) RUChCl0W, B) RUChCl11W, C) RUChCl32W, and D) RUChCl97W. **Bottom panel:** Partial RDFs obtained by Hammond et al. are included for comparison. Data were reproduced with permission from reference 29 of main text. Copyright ©, Royal Society of Chemistry.

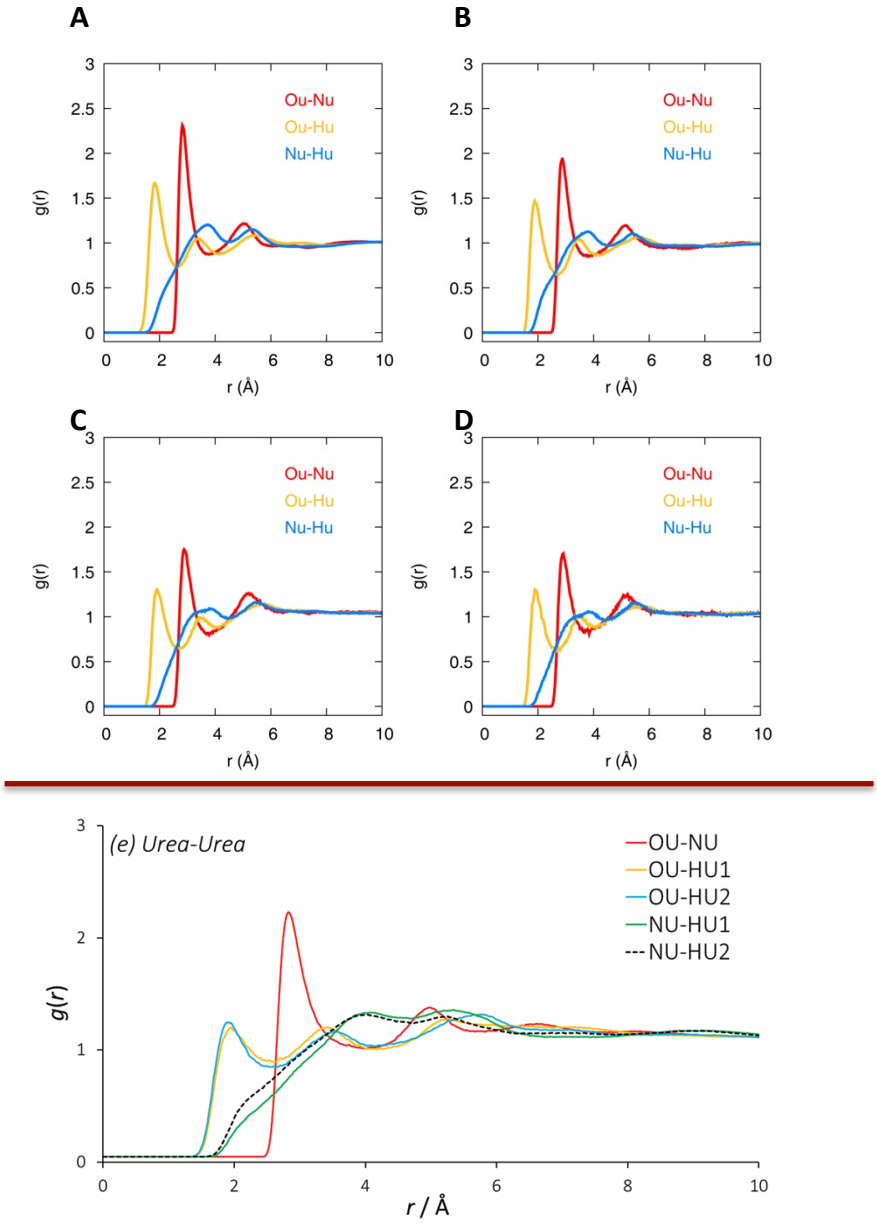

Figure S6 – Top panel: EPSR-derived partial RDFs for atom-atom pair correlations – i.e. between urea and choline atoms – in A) RUChCl0W, B) RUChCl11W, C) RUChCl32W, and D) RUChCl97W. **Bottom panel:** Partial RDFs obtained by Hammond et al. are included for comparison. Data were reproduced with permission from reference 29 of main text. Copyright ©, Royal Society of Chemistry.

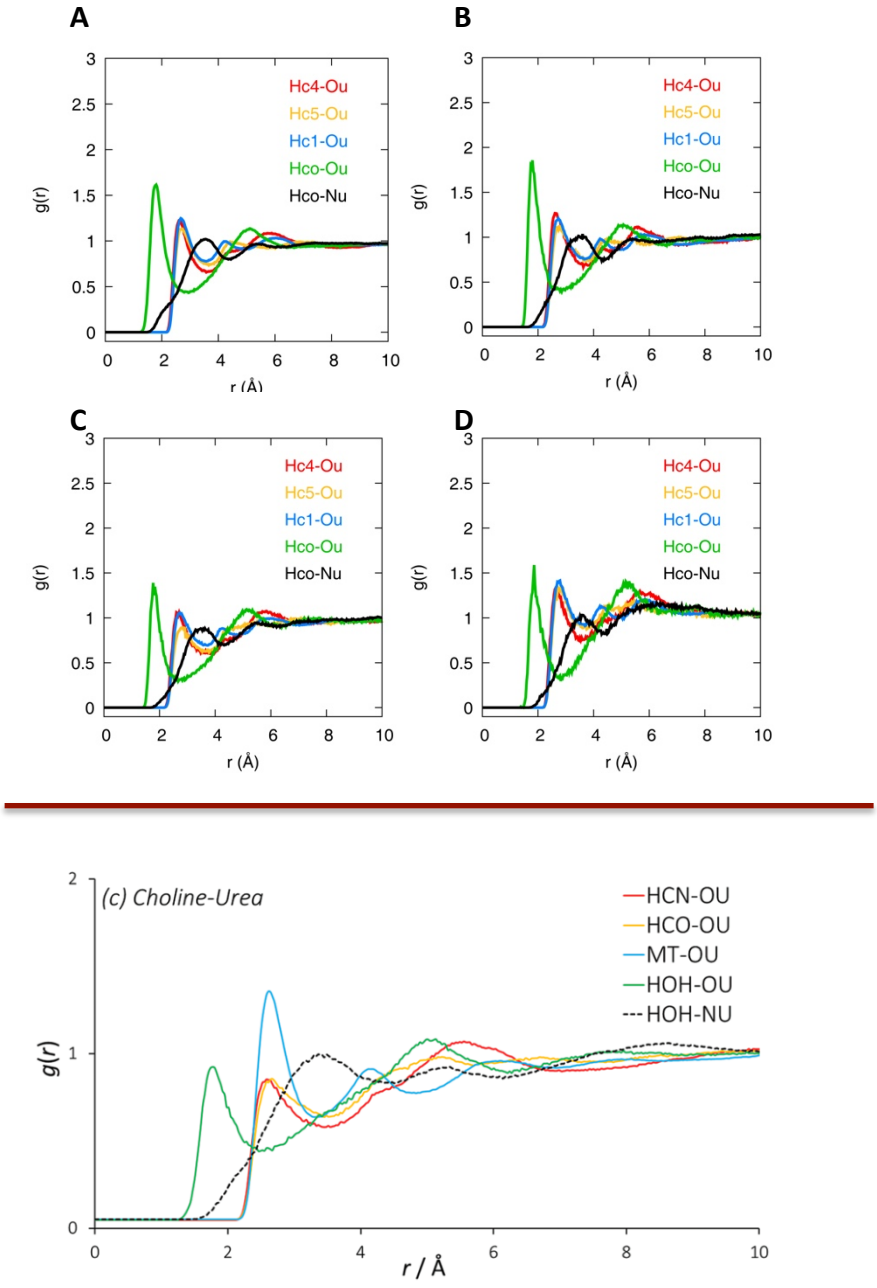

Figure S7 – Top panel: EPSR-derived partial RDFs for atom-atom pair correlations – i.e. between choline atoms and chloride – in A) RUChCl0W, B) RUChCl11W, C) RUChCl32W, and D) RUChCl97W. **Bottom panel:** Partial RDFs obtained by Hammond et al. are included for comparison. Data were reproduced with permission from reference 29 of main text. Copyright ©, Royal Society of Chemistry.

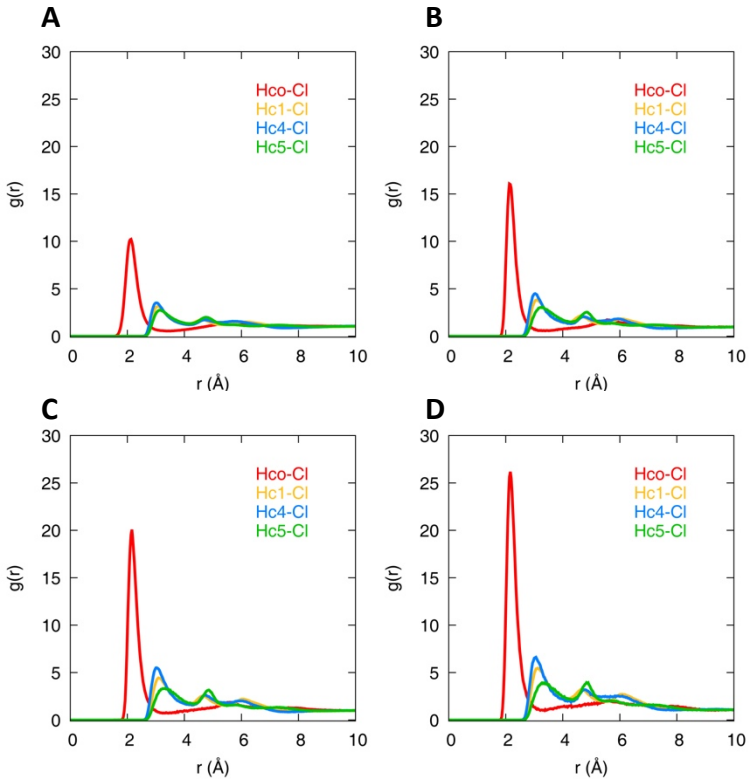

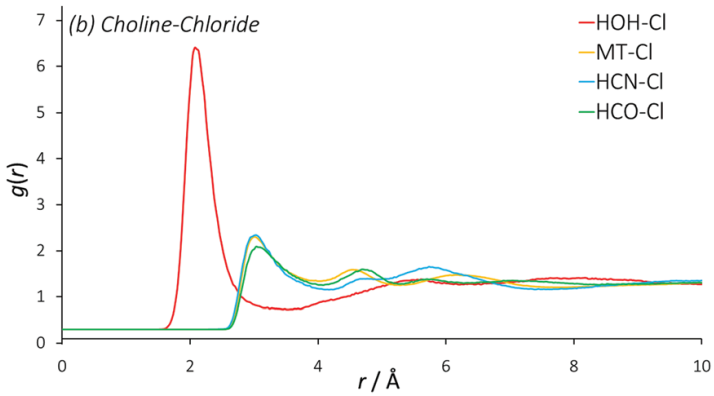

Figure S8 – Top panel: EPSR-derived partial RDFs for atom-atom pair correlations – i.e. self-correlation between choline atoms – in A) RUChCl0W, B) RUChCl11W, C) RUChCl32W, and D) RUChCl97W. **Bottom panel:** Partial RDFs obtained by Hammond et al. are included for comparison. Data were reproduced with permission from reference 29 of main text. Copyright ©, Royal Society of Chemistry.

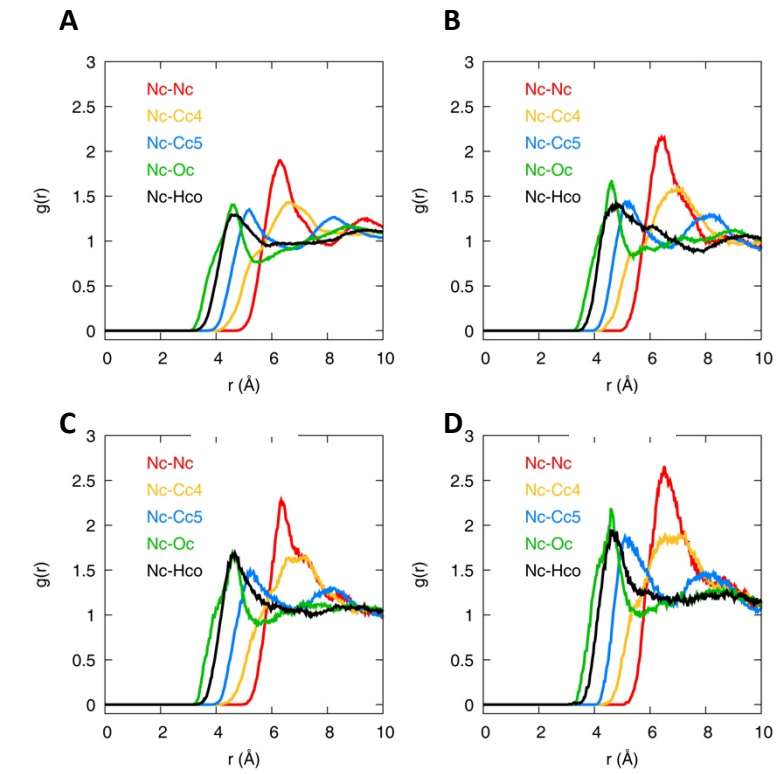

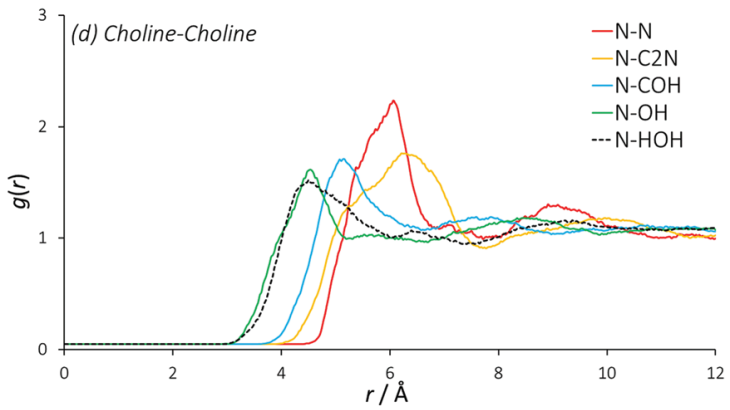

Figure S9 – EPSR-derived partial RDFs for atom-atom pair correlations – i.e. between resorcinol and urea, choline and water atoms, as well as self-correlation between resorcinol atoms – RUChCl0W (red line), RUChCl11W (green line), RUChCl32W (blue line), and RUChCl97W (yellow line).

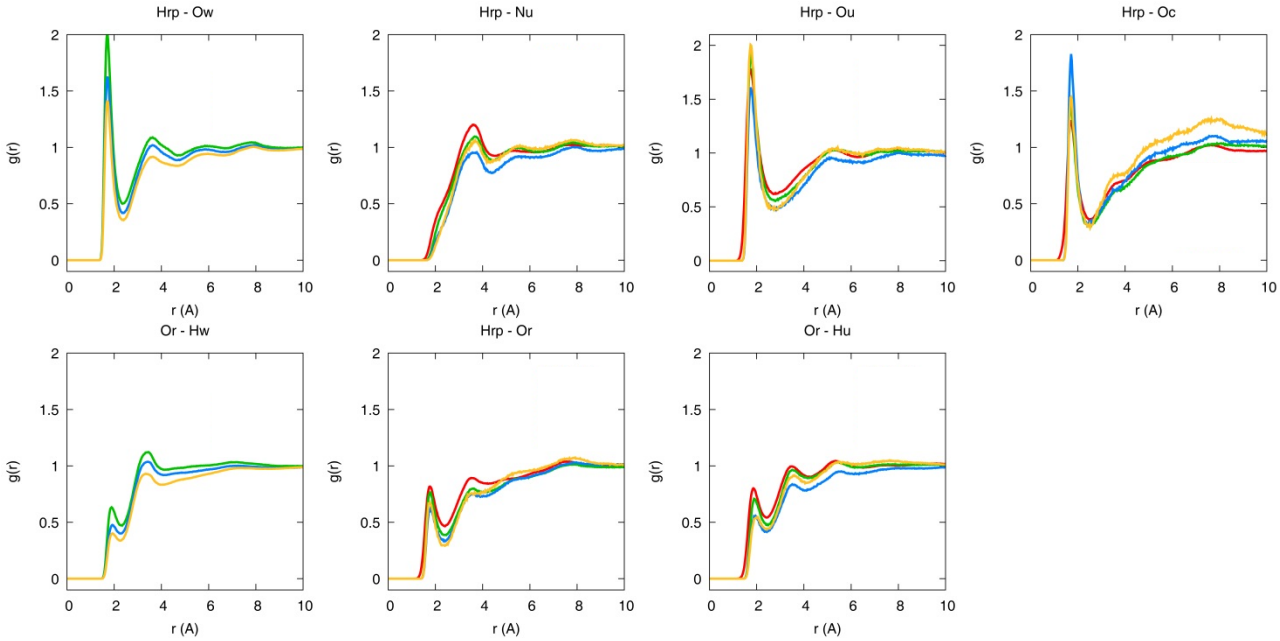

Figure S10 – EPSR-derived RDFs for pair correlations between water and all RUChCl components in RUChCl11W (green line), RUChCl32W (blue line), and RUChCl97W (yellow line).

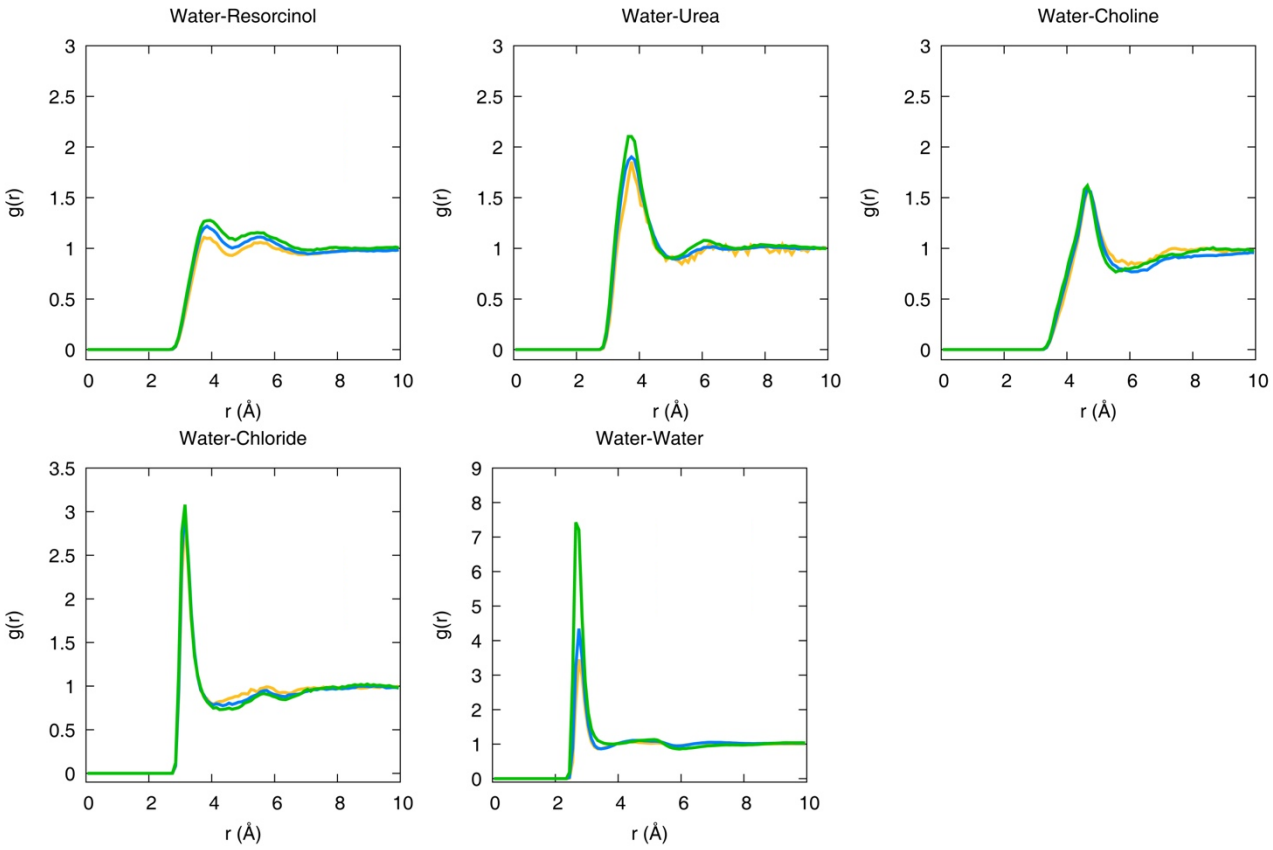

Figure S11 – EPSR-derived partial RDFs for atom-atom pair correlations between water and resorcinol, urea and choline atoms in RUChCl11W (green line), RUChCl32W (blue line), and RUChCl97W (yellow line).

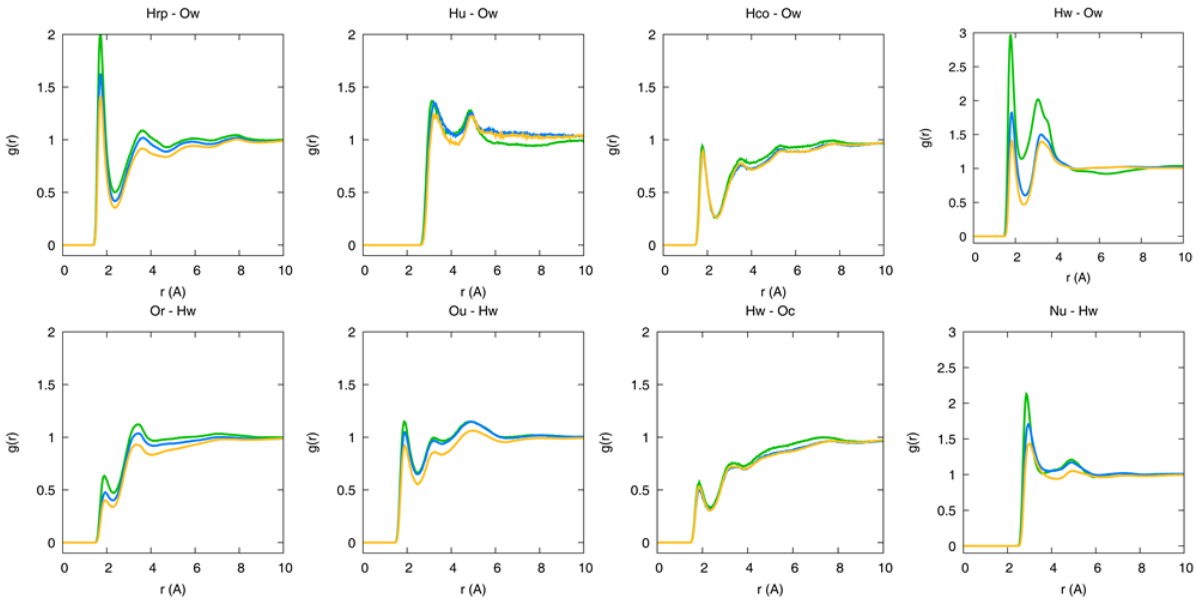

Figure S12 – EPSR-derived RDFs for different pair correlations between urea, choline and chloride in RUChCl0W (red line), RUChCl11W (green line), RUChCl32W (blue line), and RUChCl97W (yellow line).

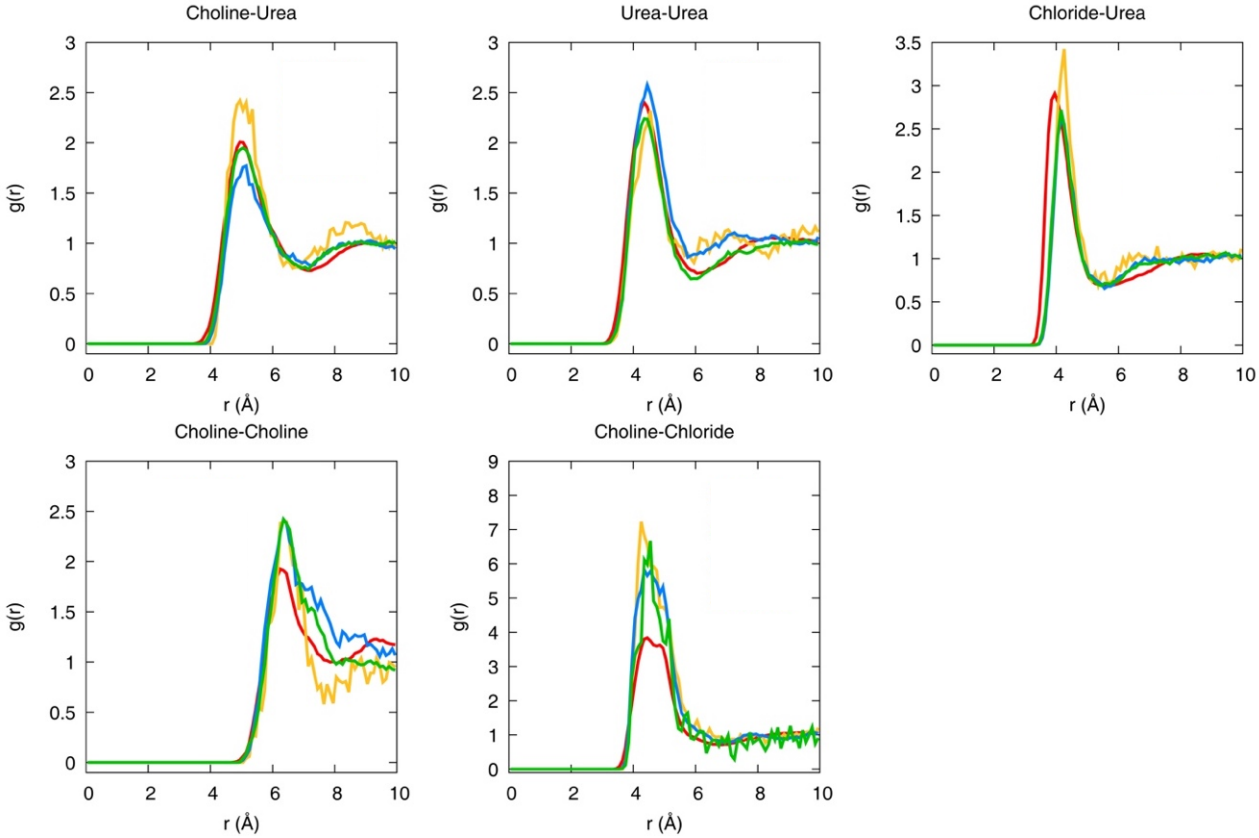

Figure S13 – EPSR-derived RDFs for different pair correlations between resorcinol and urea and choline atoms, as well as self-correlation between resorcinol atoms in RUChCl0W (red line), RUChCl11W (green line), RUChCl32W (blue line), and RUChCl97W (yellow line).

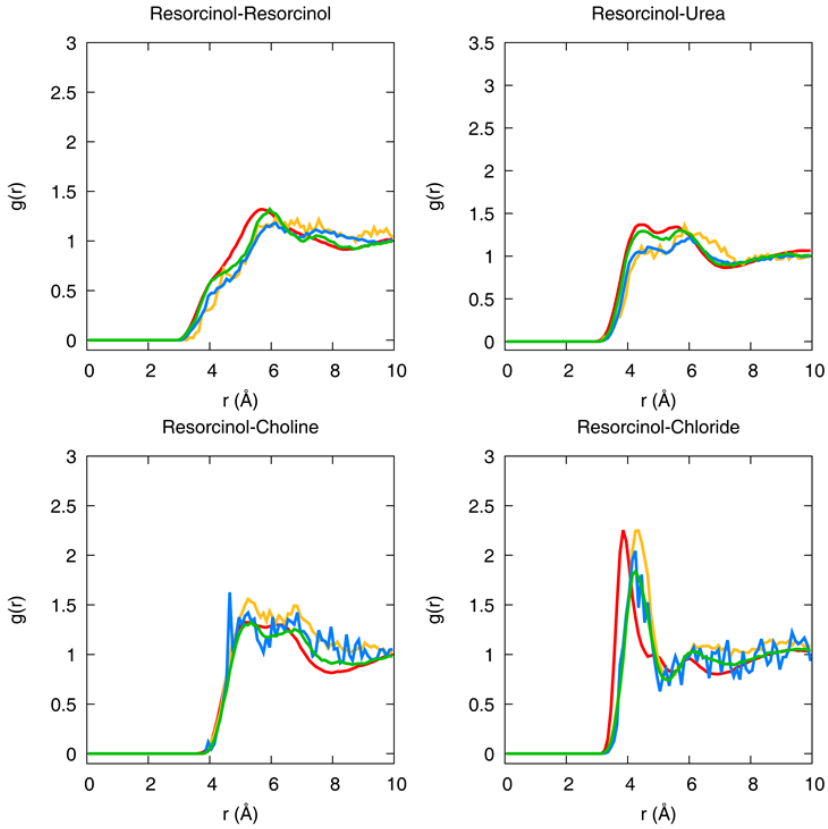

Figure S14 – EPSR SDF reconstructions of the g(r) data for atom–atom correlations between chloride and all the other DES components, including water in DES dilutions (R in dark blue, U in yellow, Ch in light blue, Cl in light purple, and W in green).

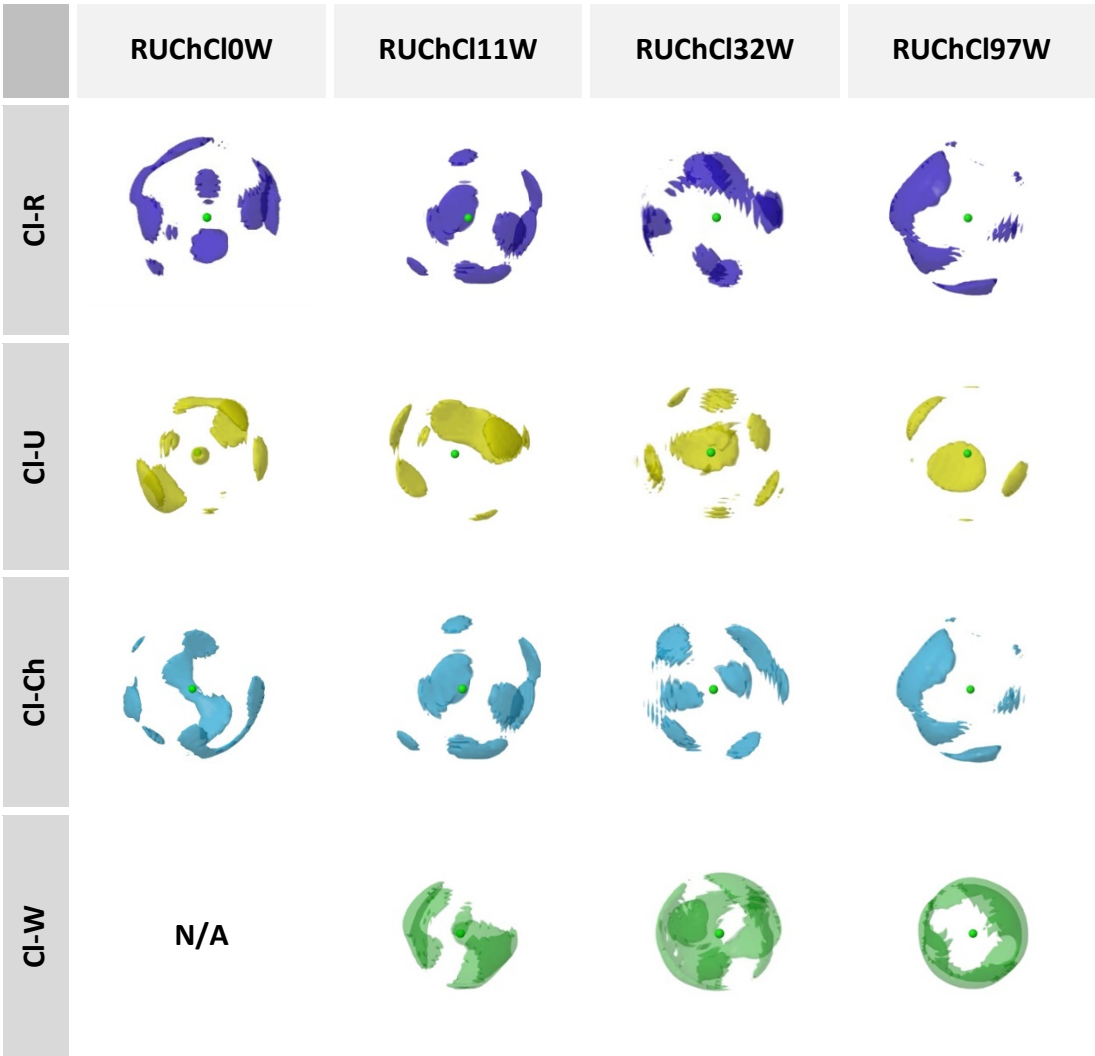

Figure S15 – EPSR SDF reconstructions of the g(r) data for atom–atom correlations between urea and all the other DES components, including W in DES dilutions (R in dark blue, U in yellow, Ch in light blue, Cl in light purple, and W in green).

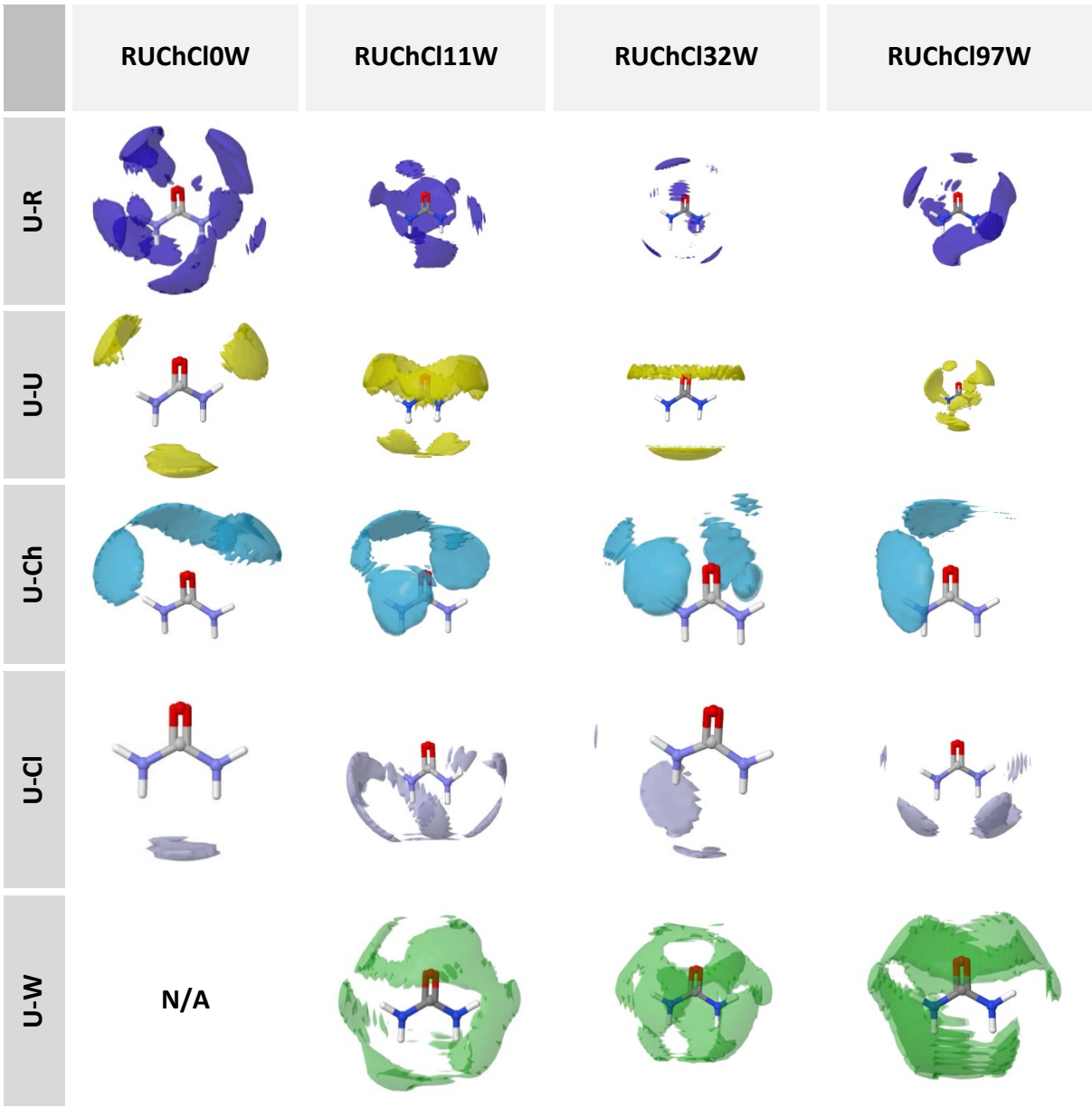

Figure S16 – Spatial density functions (SDFs) showing probabilistic 3D structures of all the components around resorcinol (R in dark blue, U in yellow, Ch in light blue, Cl in light purple, and W in green).

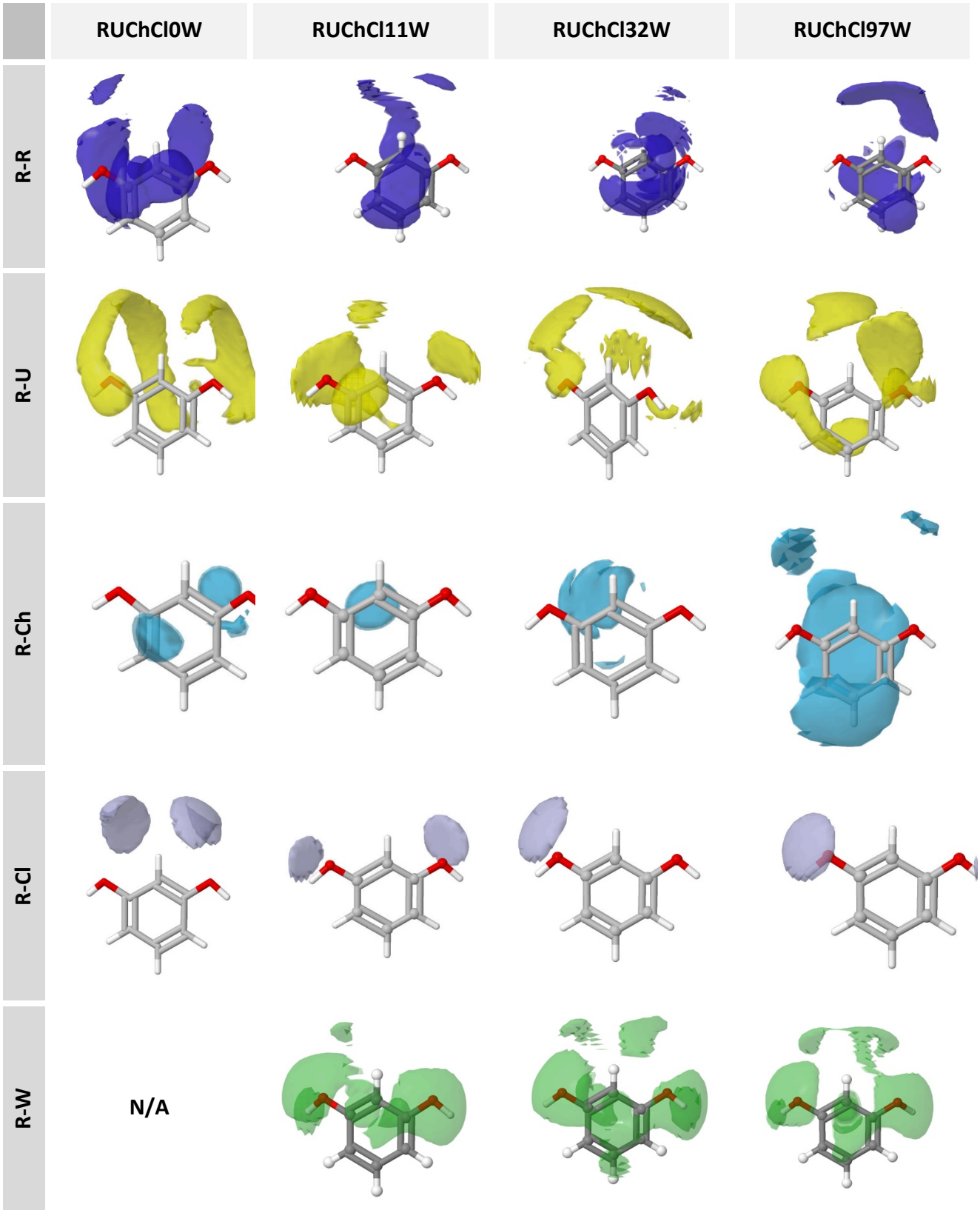

Figure S17 – EPSR SDF reconstructions of the g(r) data for atom–atom correlations between water and all the other DES components in DES dilutions (R in dark blue, U in yellow, Ch in light blue, Cl in light purple, and W in green).

	RUChCl0W	RUChCl11W	RUChCl32W	RUChCl97W
W-R	-	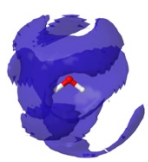	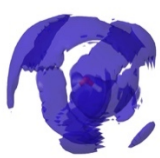	
W-U	-	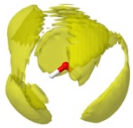		
W-Ch	-			
W-Cl	-			
W-W	-			

Figure S18 – Plot of coordination numbers (N_{coord}) versus DES content (in n, number of moles of W per mol of DES) in (a) reline-0W (100 wt% in DES content), reline-1W (93.5 wt% in DES content), reline-2W (89 wt% in DES content), reline-5W (76 wt% in DES content), reline-10W (59 wt% in DES content), reline-15W (49 wt% in DES content), reline-20W (42 wt% in DES content), and reline-30W (32.5 wt% in DES content), and (b) RUChCl0W (100 wt% in DES content), RUChCl11W (75 wt% in DES content), RUChCl32W (50 wt% in DES content), and RUChCl97W (25 wt% in DES content). Blue diamonds correspond to Cl-Hu and red squares to Cl-Hco in both reline and RUChCl, whereas green triangles squares correspond to Cl-Hrp in RUChCl.

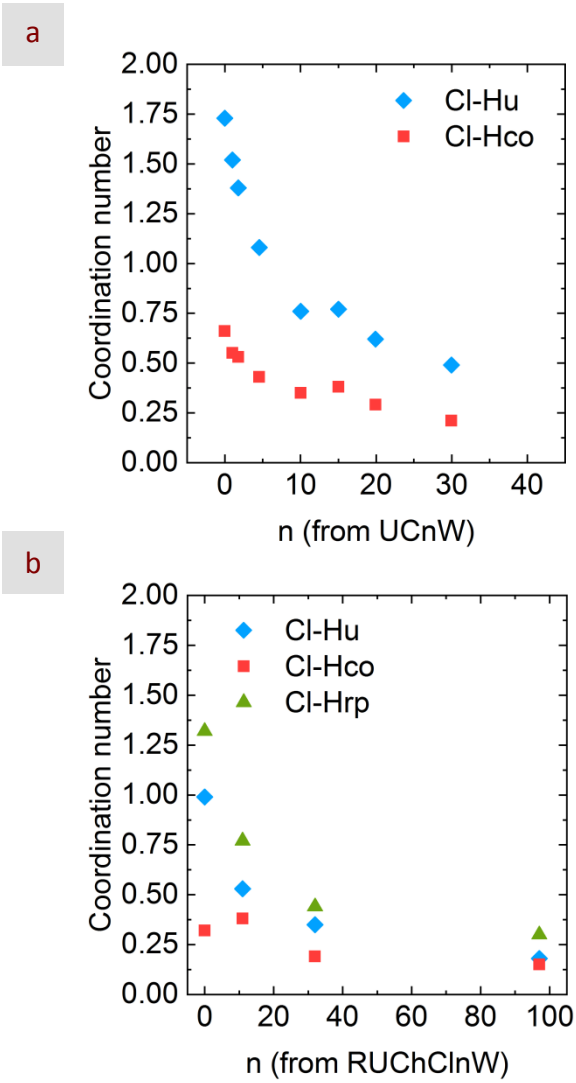

Figure S19 – Plot of self-diffusion coefficients of R (solid inverted orange triangles), U (solid purple squares), Ch (solid gray triangles) and HDO (open blue circles) versus DES content (in wt%), as obtained from NMR spectroscopy of RUChCl0W (100 wt%), RUChCl6W (85 wt%), RUChCl8W (80 wt%), RUChCl11W (75 wt%), RUChCl18W (65 wt%), RUChCl22W (60 wt%), RUChCl32W (50 wt%), RUChCl49W (40 wt%), RUChCl97W (25 wt%), and RUChCl294W (10 wt%) at (a) 25 and (c) 80 °C and from MD simulations at (b) 25 and (d) 80 °C.

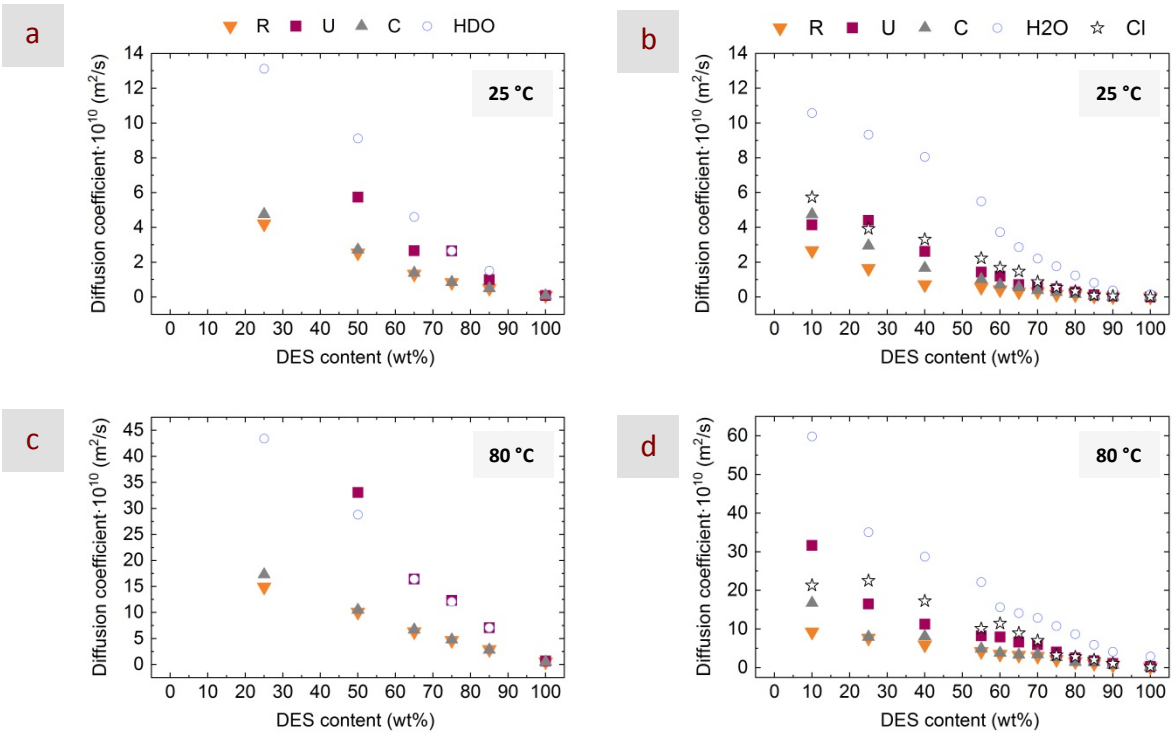

Figure S20 – (a) Plot of hypersonic (from Brillouin spectroscopy, blue circles) and ultrasonic velocity (orange circles) versus DES content (in wt%) for RUChCl0W (100 wt%), RUChCl6W (85 wt%), RUChCl8W (80 wt%), RUChCl11W (75 wt%), RUChCl18W (65 wt%), RUChCl22W (60 wt%), RUChCl32W (50 wt%), RUChCl49W (40 wt%), RUChCl97W (25 wt%), and RUChCl294W (10 wt%) at (a) 25 and (b) 80 °C.

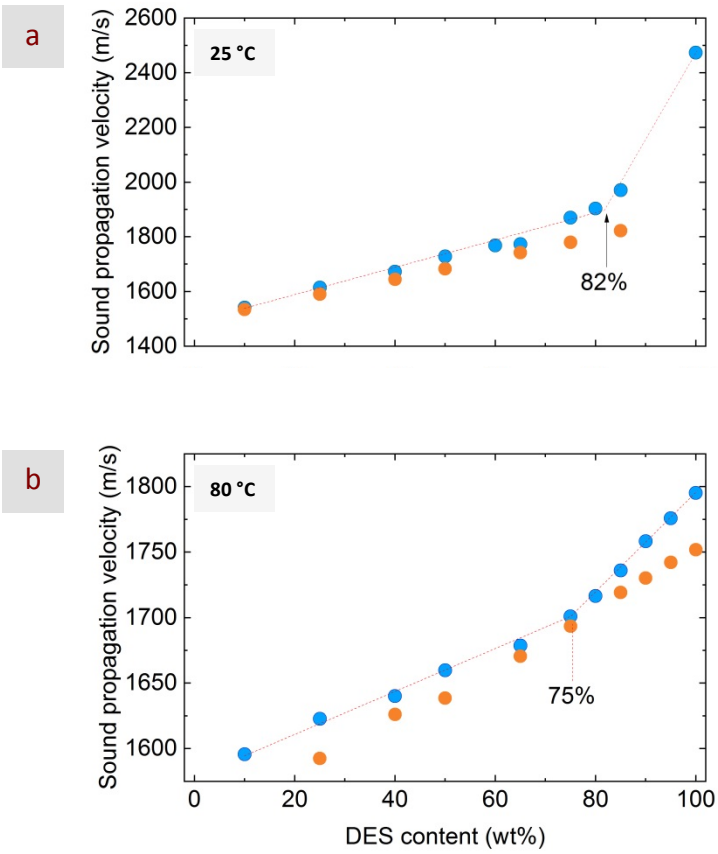

Figure S21 – Density of RUChCl and its respective aqueous dilutions at both 25 and 80°C obtained experimentally and from MD simulations.

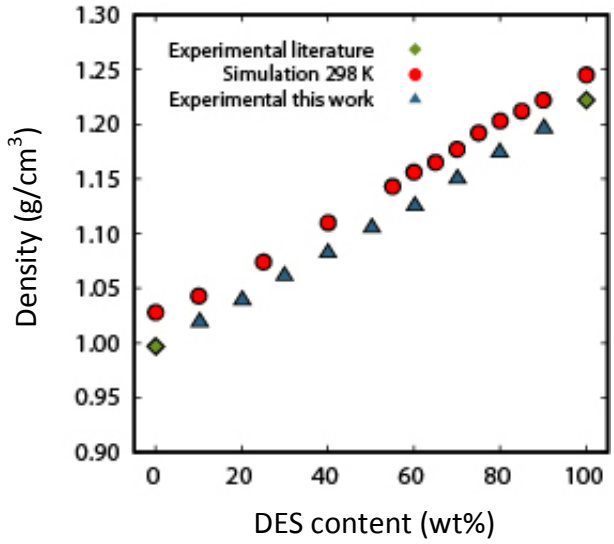

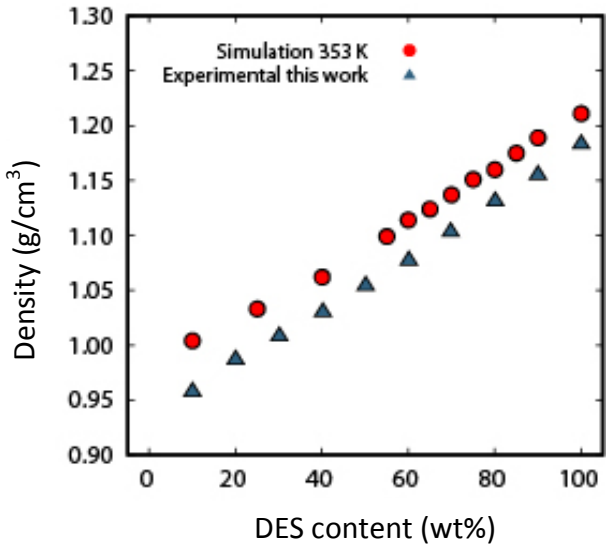

Figure S22 – Plot of self-diffusion coefficients of resorcinol (R, solid inverted orange triangles), urea (U, solid purple squares), choline (C, solid gray triangles) and HDO (open blue circles) obtained from NMR spectroscopy versus viscosity of different RUChCl aqueous solutions at (a) 25 and (b) 80 °C.

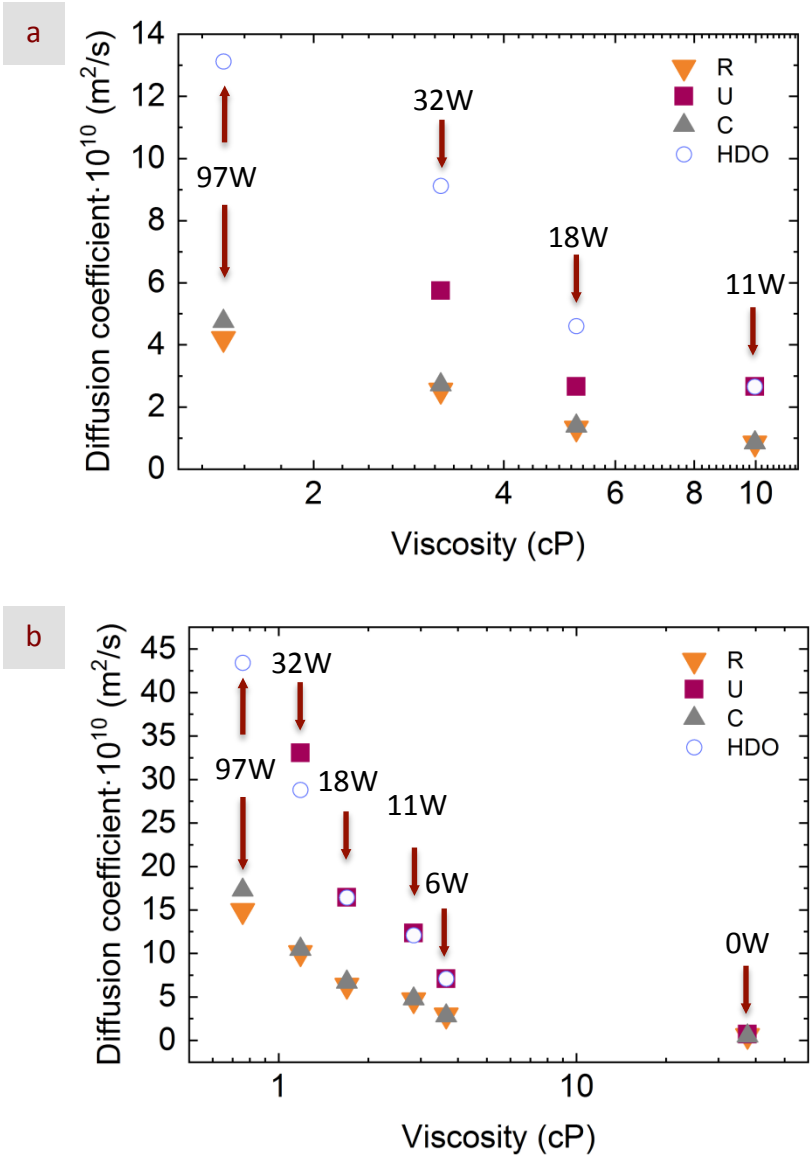

Figure S23 – Evolution of the ^{1}H NMR chemical shift of the HDO peak along with the DES content in RUChCl6W (85 wt%), RUChCl11W (75 wt%), RUChCl18W (65 wt%), RUChCl32W (50 wt%), and RUChCl97W (25 wt%) at 25 (blue) and 80 (red) °C.

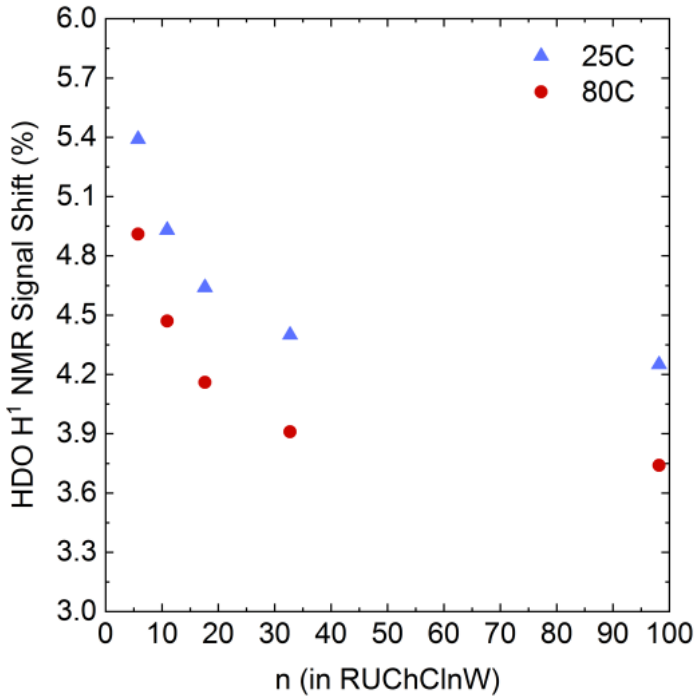

Figure S24 – ^{1}H NMR spectra of RUChCl0W, RUChCl6W, RUChCl11W, RUChCl18W, RUChCl32W, and RUChCl97W obtained at 25 °C.

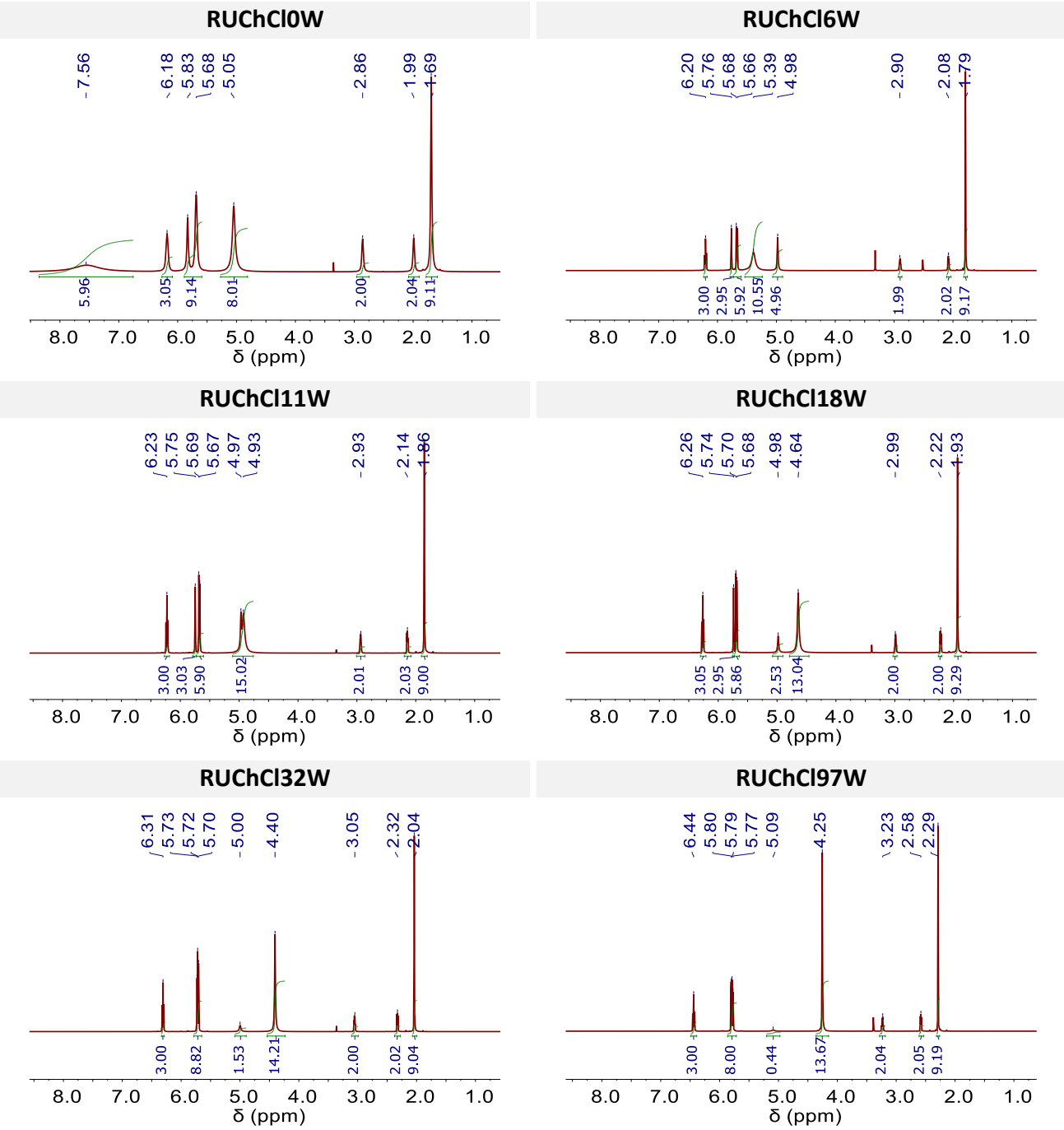

Figure S25 – ^{1}H NMR spectra of RUChCl0W, RUChCl6W, RUChCl11W, RUChCl18W, RUChCl32W, and RUChCl97W obtained at 80 °C.

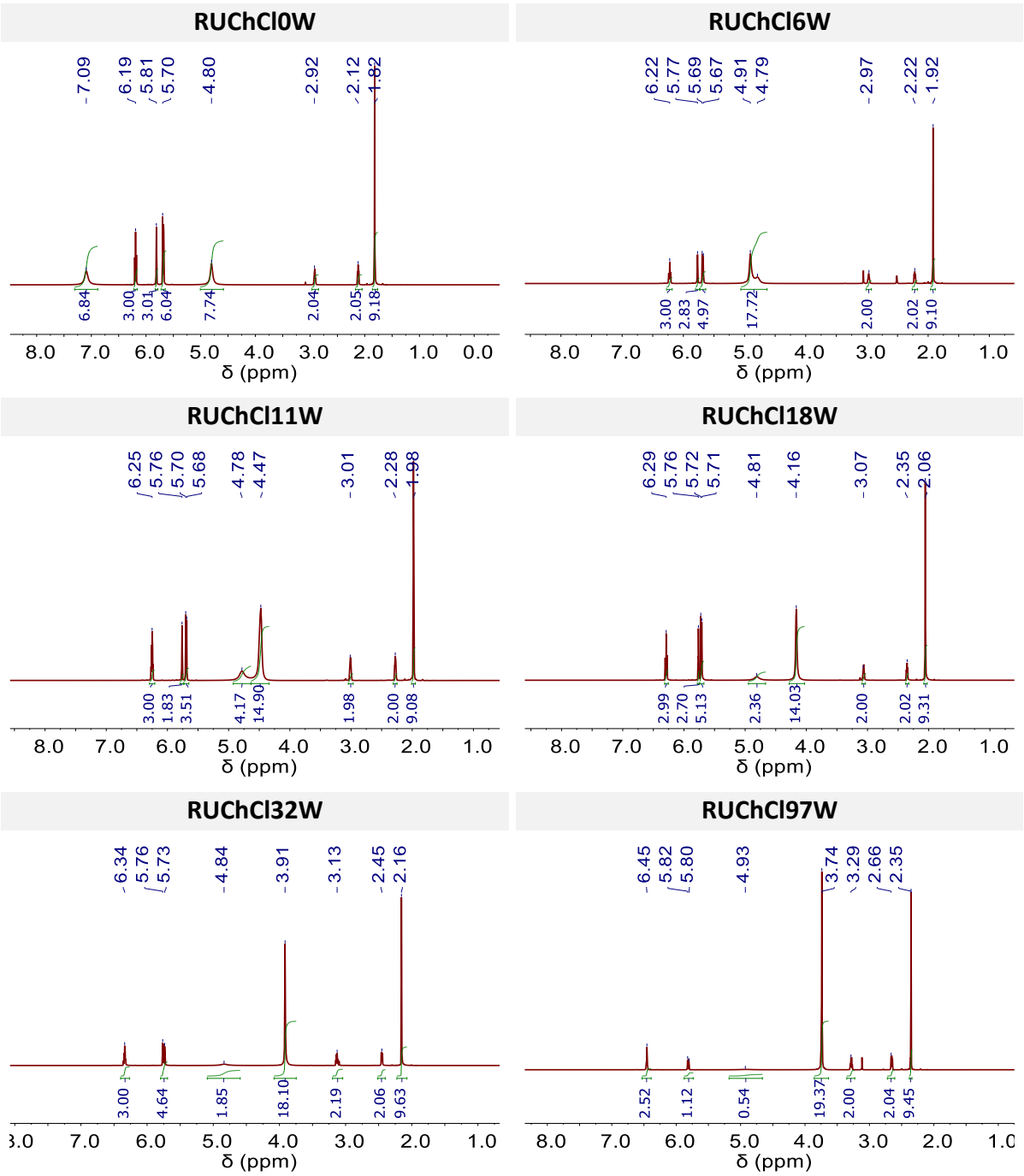

Figure S26 – DSCs scans (heating ramp in upper panel; heating and cooling ramp in lower one) of RUChCl and its respective aqueous dilutions; RUChCl0W (100 wt% in DES content, green line), RUChCl6W (85 wt% in DES content, orange line), RUChCl11W (75 wt% in DES content, red line), RUChCl18W (65 wt% in DES content, black line), RUChCl32W (50 wt% in DES content, grey line), RUChCl49W (40 wt% in DES content, blue line), and RUChCl97W (25 wt% in DES content, purple line). DSCs scans (heating ramp in upper panel, cooling ramp in lower one) of reline and malicine, and their respective aqueous dilutions are also depicted.

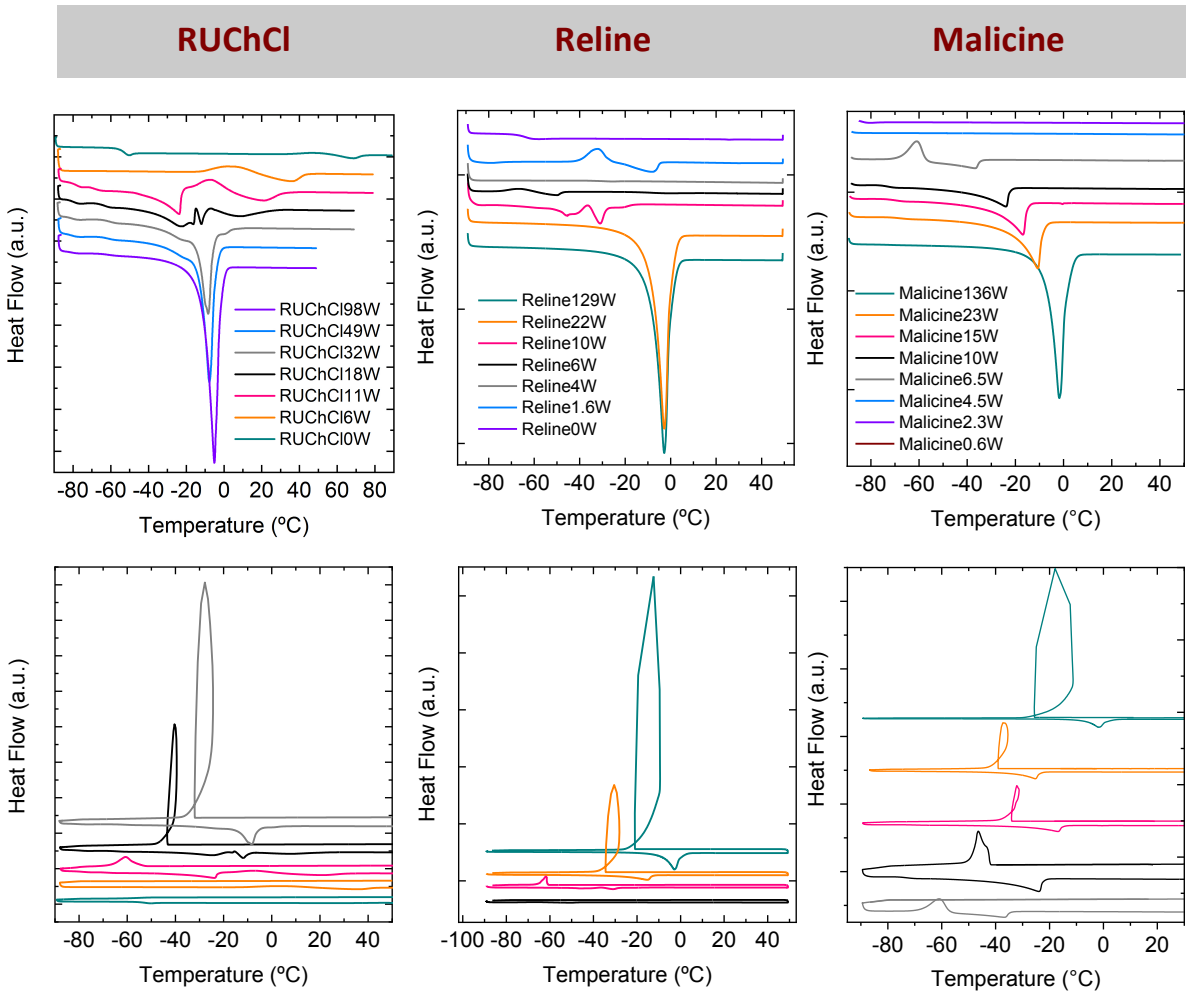

References

1 J. R. Sandercock, Trends in Brillouin scattering: studies of opaque materials, supported films, and centralmodes, in: M. Cardona, G. Güntherodt (Eds.), Light Scattering in Solids III: Recent Results, Springer Berlin Heidelberg, Berlin, Heidelberg **1982**, pp. 173–206.

2 J. K. Küger in: H. Bässler (Ed.), Optical Techniques to Characterize Polymer Systems in Studies in Polymer Science, Elsevier, Amsterdam **1989**, pp. 429–534.

3 See STE + LED + BP in http://triton.iqfr.csic.es/guide/tutorials/diff/ledbp2s.html

4 E.O. Stejskal, J.E. Tanner, Spin diffusion measurements: spin echoes in the presence of a time-dependent field gradient. *J. Chem. Phys*. **1965**, *42*, 288–292.

5 A. K. Soper, Empirical Potential Structure Refinement - EPSRshell: a user's guide. Version 18 - May 2011, RAL Technical Reports RAL-TR-2011-012. 2011.

6 S. Callear, EPSRgui manual, RAL Technical Reports RAL-TR-2017-002. STFC, 2017.

7 A. K. Soper, GudrunN and GudrunX: programs for correcting raw neutron and X-ray diffraction data to differential scattering cross section, RAL Technical Reports RAL-TR-2011-013. 2011.

8 O. S. Hammond, D. T. Bowron and K. J. Edler, Liquid structure of the choline chloride-urea deep eutectic solvent (reline) from neutron diffraction and atomistic modeling. *Green Chem.*, **2016**, *18*, 2736–2744.

9 W. L. Jorgensen, D. S. Maxwell, J. Tirado-Rives, Development and testing of the OPLS all-atom force field on conformational energetics and properties of organic liquids. *J. Am. Chem. Soc.*, **1996**, *118*, 11225–11236

10 M. Hussain, J. Anwar, The Riddle of Resorcinol Crystal Growth Revisited: Molecular Dynamics Simulations of α-Resorcinol Cristal-Water Interface. *J. Am. Chem. Soc.*, **1999**, *121*, 8583–8591.

11 S. L. Perkins, P. Painter, C. M. Colina, Molecular Dynamic Simulations and Vibrational Analysis of an Ionic Liquid Analogue. *J. Phys. Chem. B* **2013**, *117*, 10250-10260.

12 W. L. Jorgensen, N. A. McDonald, Development of an All-Atom Force Field for Heterocycles. Properties of Liquid Pyridine and Diazenes. *J. Mol. Struct.* **1998**, *424*, 145-155.

13 P. G. Kusalik, I. M. Svishchev, The Spatial Structure in Liquid Water. *Science* **1994**, *265*, 1219.

14 U. Essmann, L. Perera, M. L. Berkowitz, T. Darden, H. Lee, L. G. Pedersen, A Smooth Particle Mesh Ewald Method. *J. Chem. Phys.* **1995**, *103*, 8577-8593.

15 T. Darden, D. York, L. Pedersen, Particle Mesh Ewald - an N.Log(N) Method for Ewald Sums in Large Systems. *J. Chem. Phys.* **1993**, *98*, 10089-10092.

16 L. Martinez, R. Andrade, E. G. Birgin, J. M. Martinez, Packmol: A Package for Building Initial Configurations for Molecular Dynamics Simulations. *J. Comput. Chem.* **2009**, *30*, 2157-2164.

17 M. C. Payne, M. P. Teter, D. C. Allan, T. A. Arias, J. D. Joannopoulos, Iterative Minimization Techniques for Ab Initio Total-Energy Calculations: Molecular Dynamics and Conjugate Gradients. *Rev. Mod. Phys.* **1992**, *64*, 1045-1097.

18 G. J. Martyna, M. E. Tuckerman, D. J. Tobias, M. L. Klein, Explicit Reversible Integrators for Extended Systems Dynamics. *Mol. Phys.* **1996**, *87*, 1117-1157.

19 S. Nose, A Molecular Dynamics Method for Simulations in the Canonical Ensemble (Reprinted from Molecular Physics, Vol 52, Pg 255, 1984). *Mol. Phys.* **2002**, *100*, 191-198.

20 W. G. Hoover, Canonical Dynamics - Equilibrium Phase-Space Distributions. *Phys. Rev. A* **1985**, *31*, 1695-1697.

21 S. Pronk, et al., Gromacs 4.5: A High-Throughput and Highly Parallel Open Source Molecular Simulation Toolkit. *Bioinformatics* **2013**, *29*, 845-854.

22 B. Hess, Gromacs 4: Algorithms for Highly Efficient, Load-Balanced, and Scalable Molecular Simulation. *Abstr. of Papers of J. Am. Chem. Soc.* **2009**, *237*, 435-447.

23 H. J. C. Berendsen, D. van der Spoel, R. Vandrunen, Gromacs - a Message-Passing Parallel Molecular-Dynamics Implementation. *Comput. Phys. Commun.* **1995**, *91*, 43-56.

24 D. van der Spoel, E. Lindahl, B. Hess, G. Groenhof, A. E. Mark, H. J. C. Berendsen, Gromacs: Fast, Flexible, and Free. *J. Comput. Chem.* **2005**, *26*, 1701-1718.

25 Vicent-Luna, J. M.; Azaceta, E.; Hamad, S.; Ortiz-Roldán, J. M.; Tena-Zaera, R.; Calero, S.; Anta, J. A., Molecular Dynamics Analysis of Charge Transport in Ionic-Liquid Electrolytes Containing Added Salt with Mono, Di, and Trivalent Metal Cations. *ChemPhysChem*. **2018**, *19*, 1665-1673.

26 Vicent-Luna, J. M.; Ortiz-Roldan, J. M.; Hamad, S.; Tena-Zaera, R.; Calero, S.; Anta, J. A., Quantum and Classical Molecular Dynamics of Ionic Liquid Electrolytes for Na/Li-Based Batteries: Molecular Origins of the Conductivity Behavior. *ChemPhysChem* **2016**, *17*, 2473-81.

27 A. Luzar, D. Chandler, Structure and Hydrogen-Bond Dynamics of Water-Dimethyl Sulfoxide Mixtures by Computer-Simulations. *J. Chem. Phys.* **1993**, *98*, 8160-8173.